*Mineral. Soc. Amer. Spec. Pap.* **2**, 163–177 (1969).

# SYNTHESIS AND STABILITY OF FERRI-DIOPSIDE

H. G. HUCKENHOLZ,[1] J. FRANK SCHAIRER, AND H. S. YODER, JR.
*Geophysical Laboratory, Carnegie Institution of Washington, Washington, D.C. 20008*

## ABSTRACT

The solid solution of ferric iron in Na-free clinopyroxene was studied by crystallizing a series of compositions in the plane $CaMgSi_2O_6$-$CaSiO_3$-$Fe_2O_3$ prepared along the joins $CaMgSi_2O_6$-$CaFe_2^{3+}SiO_6$, $CaMgSi_2O_6$-$Ca_3Fe_2^{3+}Si_3O_{12}$, and $CaMgSi_2O_6$-$Fe_2O_3$, as well as some additional points in the plane. The stable phases obtained by the method of quenching at 1 atm are pseudowollastonite, hematite, and solid solutions of clinopyroxene, andradite, wollastonite, and magnetite. The maximum solid solution of the ferri-Tschermak's molecule ($CaFe_2^{3+}SiO_6$) in diopside is 33% by weight at 1175°C and that of hematite in diopside, 7% at 1292°C. Andradite is stable only in the subsolidus region; it starts to decompose at 1137° ± 5°C. Unit-cell parameters of the clinopyroxene and andraditic garnet solid solutions are given. Natural ferri-diopsides are found in igneous rocks that have undergone strongly oxidizing conditions. They contain small amounts of alkalis and have potassic affinities.

## INTRODUCTION

The principal end members of the Ca-rich clinopyroxenes in alkali basalts and their derivatives are diopside ($CaMgSi_2O_6$), hedenbergite ($CaFe^{2+}Si_2O_6$), acmite ($NaFe^{3+}Si_2O_6$), jadeite ($NaAlSi_2O_6$), and Tschermak's "molecules." Compared with the first four, a larger degree of compositional complexity is found in the Tschermak's molecules; various combinations of the main divalent ($Ca,Mg,Fe^{2+}$) and trivalent ($Al,Fe^{3+}$) or even tetravalent ($Ti^{4+}$) cations are possible. Such combinations as $CaAl_2SiO_6$, $CaTiAl_2O_6$, and probably $MgAl_2SiO_6$ are among the most common that occur in the Ca-rich clinopyroxenes of alkaline rocks. In most of those pyroxenes bearing Tschermak's molecules, a remarkable amount of $Fe^{3+}$ is also present, especially when the $Na_2O$ content is relatively small; that is, most of these clinopyroxenes have much higher amounts of ferric iron than that required to form acmite. This is demonstrated in a plot of $Na_2O$ versus $Fe_2O_3$ in Figure 1. The presence of a ferri-Tschermak's molecule $CaFe^{3+}Fe^{3+}SiO_6$ (abbreviated FTs) is inferred in which $Fe^{3+}Fe^{3+}$ occupies the sites of MgSi in the diopside structure. It was the purpose of this study to verify the inferred nature of $Fe^{3+}$ substitution in diopside and determine its extent at 1 atmosphere.

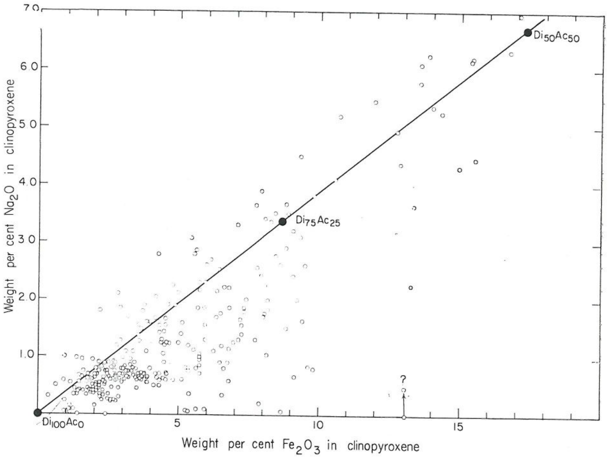

FIG. 1. Plot of $Na_2O$ versus $Fe_2O_3$ of Ca-rich clinopyroxenes from alkali basalt and their derivatives. Data were taken from Alfani, 1934; Aoki, 1964; Boesen, 1964; Boettcher, 1967; Brousse, 1961; Brousse and Boyer, 1965; von Eckermann, 1966; Erickson and Blade, 1963; Frechen, 1963; Gold, 1966; Huckenholz, 1965*a*, 1965*b*, and seven unpublished analyses; Kashkai, 1944; King, 1949; Larsen, 1942; LeMaitre, 1962; Lewis, 1967; Lupanova, 1934; Müller, 1936; Putman, 1942; Simpson, 1954; Taylor *et al.*, 1967; Tilley and Gittins, 1961; Tyler and King, 1967; Vilminot, 1965; Wilkinson, 1957, 1966; Wimmenauer, 1962; Yagi, 1953, 1966; Yoder and Tilley, 1962.

## EXPERIMENTAL PROCEDURES AND RESULTS

A series of compositions in the plane diopside ($CaMgSi_2O_6$)-wollastonite ($CaSiO_3$)-hematite ($Fe_2O_3$) in the quaternary system $CaO$-$MgO$-$Fe_2O_3$-$SiO_2$ (Fig. 2) were prepared along the joins diopside–ferri-Tschermak's molecule, diopside-andradite, and diopside-hematite, as well as some additional points in this plane. The data in the present investigation were obtained by means of the quenching method, first employed by Shepherd and Rankin (1909), and were collected at 1 atm pressure in the temperature range 1000° to 1500°C. The results are presented in three *T-X* diagrams and in four isothermal sections of the di-wo-hem plane on the basis of 268 critical runs, compiled in Table 1. The products formed in the experiments were identified by optical determinations and powder X-ray diffraction patterns, as well as by microprobe analyses. Phases encountered in the runs are glass, pseudowollastonite, hematite, and solid solutions of clinopyroxene, wollastonite, magnetite, and andradite, all of which are described briefly below.

*Description of phases.* Colorless to light-brown glasses are quenched from melts above liquidus temperatures when the bulk compositions of the mixtures have low contents of ferric iron. The color of the glass changes continuously to a darker brown when the iron content in the mixtures is increased. The first appearance of glass, *i.e.* the beginning of melting of a sample completely crystallized at 1050°C, can be determined in most cases by the temperature at which the sample begins to frit. This method of determining the solidus gives, of course, only an approximate location of the beginning of melting in the *T-X* diagrams.

---

[1] Present address: Mineralogisch-Petrographisches Institut der Universität München, München, West Germany.

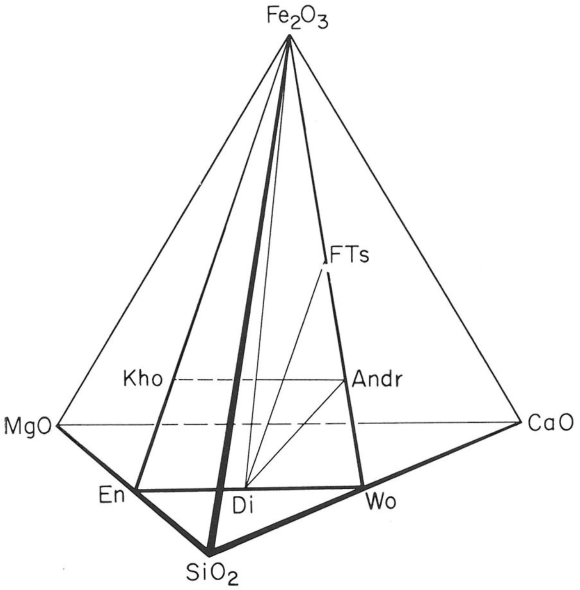

FIG. 2. The quaternary system $CaO$-$MgO$-$Fe_2O_3$-$SiO_2$ and the plane wollastonite-diopside-(enstatite)-hematite ($Fe_2O_3$). Abbreviations for phases encountered: FTs, ferri-Tschermak's molecule; Andr, andradite; Kho, khoharite; Wo, wollastonite; Di, diopside; and En, enstatite.

TABLE 1. CRITICAL QUENCHING RESULTS FOR COMPOSITIONS ON THE JOIN DIOPSIDE-WOLLASTONITE-HEMATITE

| Starting material[a] | T, °C | Time[b] | Products | Remarks |
|---|---|---|---|---|
| Composition: $di_{90}wo_{4.2}hem_{5.8}(=di_{90}FTs_{10})$ | | | | |
| xtl | 1370 | 2 h | glass | |
| xtl | 1365 | 2 h | $cpx_{ss}$+glass | small amounts of $cpx_{ss}$ |
| xtl | 1300 | 4 h | $cpx_{ss}$+glass | comp. of $cpx_{ss}$: 6±3% FTs |
| xtl | 1280 | 1 d | $cpx_{ss}$+glass | traces of glass |
| xtl | 1270 | 1 d | $cpx_{ss}$ | $cpx_{ss}$ with voids |
| xtl | 1155 | 7 d | $cpx_{ss}$ | unit-cell parameters determined |
| xtl | 1050 | 27 d | $cpx_{ss}$ | unit-cell parameters determined |
| Composition: $di_{80}wo_{8.4}hem_{11.6}(=di_{80}FTs_{20})$ | | | | |
| xtl | 1345 | 2 h | glass | |
| xtl | 1340 | 2 h | $cpx_{ss}$+glass | |
| xtl | 1240 | 19 h | $cpx_{ss}$+glass | comp. of $cpx_{ss}$: 17±2% FTs |
| xtl | 1200 | 16 d | $cpx_{ss}$ | |
| xtl | 1155 | 7 d | $cpx_{ss}$ | unit-cell parameters determined |
| xtl | 1050 | 45 d | $cpx_{ss}$ | unit-cell parameters determined |
| xtl | 900 | 54 d | $cpx_{ss}$+hem | |
| Composition: $di_{75}wo_{10.5}hem_{14.5}(=di_{75}FTs_{25})$ | | | | |
| xtl | 1335 | 2 h | glass | |
| xtl | 1330 | 3 h | $cpx_{ss}$+glass | small amounts of $cpx_{ss}$ |
| xtl | 1225 | 7 d | $cpx_{ss}$+glass | comp. of $cpx_{ss}$: 21±2% FTs |
| xtl | 1200 | 12 d | $cpx_{ss}$ | traces of glass |
| xtl | 1155 | 12 d | $cpx_{ss}$ | unit-cell parameters determined |
| xtl | 1125 | 12 d | $cpx_{ss}$ | |
| xtl | 1100 | 12 d | $cpx_{ss}$+hem | |
| xtl | 1050 | 12 d | $cpx_{ss}$+hem | very fine-grained hem |
| Composition: $di_{68.9}wo_{13.1}hem_{18}(=di_{68.9}FTs_{31.1})$ | | | | |
| xtl | 1320 | 2 h | glass | |
| xtl | 1315 | 2 h | $cpx_{ss}$+glass | rare $cpx_{ss}$ |
| xtl | 1200 | 16 d | $cpx_{ss}$+glass | comp. of $cpx_{ss}$: 24±2% FTs |
| xtl | 1170 | 7 d | $cpx_{ss}$ | |
| xtl | 1155 | 7 d | $cpx_{ss}$ | unit-cell parameters determined |
| xtl | 1150 | 27 d | $cpx_{ss}$ | |
| xtl | 1140 | 21 d | $cpx_{ss}$+hem | very rare hem |
| xtl | 1050 | 67 d | $cpx_{ss}$+hem | |
| Composition: $di_{65}wo_{14.7}hem_{20.3}(=di_{65}FTs_{35})$ | | | | |
| xtl | 1310 | 3 h | glass | |
| xtl | 1305 | 3 h | $cpx_{ss}$+glass | rare $cpx_{ss}$ |
| xtl | 1225 | 7 d | $cpx_{ss}$+hem+glass | traces of glass and hem |
| xtl | 1200 | 12 d | $cpx_{ss}$+hem+glass | |
| xtl | 1175 | 10 d | $cpx_{ss}$+hem+glass | glass in very small amounts |
| xtl | 1150 | 27 d | $cpx_{ss}$+hem | |
| xtl | 1050 | 12 d | $cpx_{ss}$+hem | |
| xtl | 900 | 54 d | $cpx_{ss}$+hem+$andr_{ss}$ | traces of $andr_{ss}$ |
| Composition: $di_{59.3}wo_{17.2}hem_{23.5}(=di_{59.3}FTs_{40.7})$ | | | | |
| xtl | 1295 | 3 h | glass | |
| xtl | 1290 | 4 h | $cpx_{ss}$+glass | |
| xtl | 1270 | 1 d | $cpx_{ss}$+$mt_{ss}$+glass | |
| xtl | 1250 | 2 d | $cpx_{ss}$+$mt_{ss}$+glass | |
| xtl | 1225 | 2 d | $cpx_{ss}$+$mt_{ss}$+glass | |
| xtl | 1220 | 4 d | $cpx_{ss}$+$mt_{ss}$+hem +glass | hem in small amounts |
| xtl | 1215 | 5 d | $cpx_{ss}$+hem+glass | |
| xtl | 1175 | 7 d | $cpx_{ss}$+hem+glass | very small amounts of glass |
| xtl | 1150 | 7 d | $cpx_{ss}$+hem | |
| xtl | 1140 | 21 d | $cpx_{ss}$+hem+$andr_{ss}$ | very rare $andr_{ss}$ |
| xtl | 1100 | 63 d | $cpx_{ss}$+hem+$andr_{ss}$ | rare $andr_{ss}$ |
| xtl | 1050 | 45 d | $cpx_{ss}$+hem+$andr_{ss}$ | unit-cell parameters of $cpx_{ss}$ determined |
| xtl | 900 | 54 d | $cpx_{ss}$+hem+$andr_{ss}$ | very rare $andr_{ss}$ |
| Composition: $di_{55.5}wo_{19}hem_{25.5}(=di_{55.5}FTs_{44.5})$ | | | | |
| glass | 1295 | 2 h | glass | |
| glass | 1290 | 2 h | $mt_{ss}$+glass | rare $mt_{ss}$ |
| glass | 1200 | 1 d | $cpx_{ss}$+hem+glass | |
| glass | 1175 | 2 d | $cpx_{ss}$+hem+$wo_{ss}$ +glass | $wo_{ss}$ in traces |
| Composition: $di_{51.6}wo_{20.4}hem_{28}(=di_{51.6}FTs_{48.4})$ | | | | |
| xtl | 1305 | 4 h | glass | |
| xtl | 1300 | 4 h | $mt_{ss}$+glass | |
| xtl | 1290 | 1 d | $mt_{ss}$+glass | comp. of $mt_{ss}$: $(Mg_{0.52}Ca_{0.04}Fe_{2.44})O_4$ |
| xtl | 1275 | 1 d | $cpx_{ss}$+$mt_{ss}$+glass | |
| xtl | 1225 | 7 d | $cpx_{ss}$+$mt_{ss}$+hem +glass | |

Primary clinopyroxene forms stout, colorless to light-yellow prisms. At lower temperatures mosaic intergrowths of grains are obtained. The color of the clinopyroxenes depends on the amount of the ferri-Tschermak's molecule dissolved in the diopside structure; $diopside_{100}FTs_0$ is colorless, $diopside_{90}FTs_{10}$ light yellow, $diopside_{80}FTs_{20}$ yellow, and $diopside_{68.9}FTs_{31.1}$ brownish yellow. Anomalous birefringence increases in the same order.

Crystals of pseudowollastonite and laths of a wollastonite solid solution crystallize as primary phases in the iron-poor portion of the di-wo-hem plane. The two phases can be distinguished by their optical properties. In the presence of iron, pseudowollastonite is colorless, optically positive, and highly birefringent, whereas the wollastonite solid solution has a slightly yellow color and is optically negative with very low birefringence.

Magnetite, which was identified in reflected light and by microprobe techniques, forms small octahedra in brown glasses when crystallized below the liquidus. Primary hematite occurs as rounded plates; hexagonal outlines are rare. Dark reddish brown absorption colors and strong anomalous birefringence may be detected in very thin plates.

Andradite appears as rounded grains showing very light-yellow colors. Faceted crystals were not observed, because several thorough grindings were necessary during the crystallizing period of at least 50 days at temperatures of 1050° or 1135°C for complete solution of all metastably formed wollastonites in the andradite. This procedure appears to inhibit the formation of completely euhedral crystals. All starting mixtures were treated in this way to accelerate equilibration. As a result, very fine-grained intergrowths of phases were formed in polyphase assemblages under subsolidus conditions.

*Oxidation state.* The plane chosen for study is not strictly ternary mainly because ferrous iron is present in amounts which depend on the temperature and composition. Complex magnetite solid solution appears as a phase in the more iron-rich part of the system at temperatures higher than 1200°C. The composition

TABLE 1—(*Continued*)

| Starting material$^a$ | T, °C | Time$^b$ | Products | Remarks |
|---|---|---|---|---|
| xtl | 1215 | 7 d | cpx$_{ss}$+mt$_{ss}$+hem +glass | |
| xtl | 1200 | 7 d | cpx$_{ss}$+hem+wo$_{ss}$ +glass | |
| xtl | 1175 | 2 d | cpx$_{ss}$+hem+wo$_{ss}$ +glass | |
| xtl | 1150 | 27 d | cpx$_{ss}$+hem+andr$_{ss}$ | |
| xtl | 1050 | 27 d | cpx$_{ss}$+hem+andr$_{ss}$ | |
| Composition: $\mathrm{di_{43}wo_{34}hem_{33}(=di_{43}FTs_{57})}$ | | | | |
| xtl | 1350 | 2 h | glass | |
| xtl | 1345 | 2 h | mt$_{ss}$+glass | very rare mt$_{ss}$ |
| xtl | 1340 | 2 h | mt$_{ss}$+glass | |
| xtl | 1300 | 3 h | mt$_{ss}$+glass | comp. of mt$_{ss}$: $\mathrm{(Mg_{0.31}Ca_{0.03}Fe_{2.66})O_4}$ |
| xtl | 1250 | 2 d | mt$_{ss}$+glass | traces of hem and cpx$_{ss}$ |
| xtl | 1235 | 3 d | cpx$_{ss}$+mt$_{ss}$+hem +glass | |
| xtl | 1225 | 7 d | cpx$_{ss}$+mt$_{ss}$+hem +glass | |
| xtl | 1200 | 7 d | cpx$_{ss}$+hem+glass | mt$_{ss}$ and wo$_{ss}$ in traces |
| xtl | 1160 | 7 d | cpx$_{ss}$+hem+wo$_{ss}$ | |
| xtl | 1150 | 14 d | cpx$_{ss}$+hem+andr$_{ss}$ | |
| glass | 1050 | 27 d | cpx$_{ss}$+hem+andr$_{ss}$ | andr$_{ss}$ $a_0=12.051\pm0.008$ Å |
| Composition: $\mathrm{di_{30}wo_{29.5}hem_{40.5}(=di_{30}FTs_{70})}$ | | | | |
| glass | 1410 | 2 h | glass | |
| glass | 1405 | 2 h | mt$_{ss}$+glass | very rare mt$_{ss}$ |
| xtl | 1380 | 2 h | mt$_{ss}$+glass | comp. of mt$_{ss}$: $\mathrm{(Mg_{0.26}Ca_{0.03}Fe_{2.71})O_4}$ |
| xtl | 1325 | 2 h | mt$_{ss}$+glass | comp. of mt$_{ss}$: $\mathrm{(Mg_{0.29}Ca_{0.02}Fe_{2.69})O_4}$ |
| xtl | 1310 | 2 h | mt$_{ss}$+hem+glass | |
| xtl | 1250 | 2 d | mt$_{ss}$+hem+glass | |
| xtl | 1235 | 2 d | mt$_{ss}$+hem+cpx$_{ss}$ +glass | cpx$_{ss}$ in traces |
| xtl | 1225 | 7 d | cpx$_{ss}$+mt$_{ss}$+hem +glass | |
| xtl | 1200 | 7 d | cpx$_{ss}$+hem+wo$_{ss}$ +glass | wo$_{ss}$ in traces |
| xtl | 1160 | 14 d | cpx$_{ss}$+hem+wo$_{ss}$ | |
| xtl | 1150 | 14 d | cpx$_{ss}$+hem+andr$_{ss}$ | |
| xtl | 1135 | 7 d | cpx$_{ss}$+hem+andr$_{ss}$ | andr$_{ss}$ $a=12.053\pm0.003$ Å |
| glass | 1050 | 86 d | cpx$_{ss}$+hem+andr$_{ss}$ | andr$_{ss}$ $a=12.053\pm0.004$ Å |
| Composition: $\mathrm{di_{20}wo_{33.7}hem_{46.3}(=di_{20}FTs_{80})}$ | | | | |
| glass | 1415 | 2 h | glass | |
| glass | 1410 | 2 h | mt$_{ss}$+glass | very rare mt$_{ss}$ |
| glass | 1360 | 1 d | mt$_{ss}$+glass | |
| glass | 1350 | 1 d | mt$_{ss}$+hem+glass | |
| xtl | 1250 | 2 d | mt$_{ss}$+hem+glass | |
| xtl | 1237 | 3 d | cpx$_{ss}$+mt$_{ss}$+hem +glass | |
| xtl | 1225 | 2 d | cpx$_{ss}$+mt$_{ss}$+hem +glass | wo$_{ss}$ in very small amounts |
| xtl | 1200 | 7 d | cpx$_{ss}$+hem+wo$_{ss}$ +glass | |
| xtl | 1175 | 7 d | cpx$_{ss}$+hem+wo$_{ss}$ +glass | glass in traces |
| xtl | 1160 | 14 d | cpx$_{ss}$+hem+wo$_{ss}$ | |
| xtl | 1150 | 14 d | cpx$_{ss}$+hem+andr$_{ss}$ | |
| xtl | 1135 | 14 d | cpx$_{ss}$+hem+andr$_{ss}$ | andr$_{ss}$ $a=12.053\pm0.005$ Å |
| glass | 1050 | 82 d | cpx$_{ss}$+hem+andr$_{ss}$ | andr$_{ss}$ $a=12.053\pm0.003$ Å |
| Composition: $\mathrm{di_{15}wo_{35.8}hem_{49.2}(=di_{15}FTs_{85})}$ | | | | |
| xtl | 1400 | 2 h | glass | |
| xtl | 1390 | 2 h | mt$_{ss}$+glass | |
| xtl | 1380 | 2 h | mt$_{ss}$+glass | |
| xtl | 1370 | 4 h | mt$_{ss}$+hem+glass | |
| xtl | 1250 | 1 d | mt$_{ss}$+hem+glass | traces of pwo |
| xtl | 1240 | 2 d | mt$_{ss}$+hem+pwo +glass | |
| Composition: $\mathrm{di_{10}wo_{27.9}hem_{62.1}(=di_{10}FTs_{90})}$ | | | | |
| glass | 1385 | 2 h | glass | |
| glass | 1380 | 3 h | hem+glass | |
| xtl | 1275 | 1 d | hem+glass | traces of pwo |
| xtl | 1250 | 2 d | hem+pwo+glass | |
| xtl | 1240 | 2 d | hem+pwo+glass | |
| xtl | 1225 | 7 d | cpx$_{ss}$+hem+wo$_{ss}$ +glass | glass in traces |

TABLE 1—(*Continued*)

| Starting material$^a$ | T, °C | Time$^b$ | Products | Remarks |
|---|---|---|---|---|
| xtl | 1200 | 14 d | cpx$_{ss}$+hem+wos$_s$ | |
| xtl | 1160 | 14 d | cpx$_{ss}$+hem+wo$_{ss}$ | |
| xtl | 1155 | 14 d | cpx$_{ss}$+hem+wo$_{ss}$ +andr$_{ss}$ | andr$_{ss}$ in very rare amounts |
| xtl | 1150 | 14 d | cpx$_{ss}$+hem+andr$_{ss}$ | |
| xtl | 1135 | 7 d | cpx$_{ss}$+hem+andr$_{ss}$ | andr$_{ss}$ $a=12.054\pm0.004$ Å |
| glass | 1050 | 78 d | cpx$_{ss}$+hem+andr$_{ss}$ | andr$_{ss}$ $a=12.054\pm0.004$ Å |
| Composition: $\mathrm{di_{0}wo_{42.1}hem_{57.9}(=di_{0}FTs_{100})}$ | | | | |
| glass | 1390 | 2 h | glass | |
| glass | 1380 | 3 h | hem+glass | |
| xtl | 1300 | 12 h | hem+glass | |
| xtl | 1290 | 12 h | hem+pwo+glass | small amounts of pwo and glass |
| xtl | 1275 | 1 d | hem+pwo | |
| xtl | 1160 | 14 d | hem+pwo | |
| xtl | 1150 | 14 d | hem+pwo+andr$_{ss}$ | |
| xtl | 1145 | 7 d | hem+pwo+andr$_{ss}$ | |
| xtl | 1135 | 14 d | hem+andr$_{ss}$ | andr$_{ss}$ $a=12.052\pm0.004$ Å |
| glass | 1050 | 100 d | hem+andr$_{ss}$ | andr$_{ss}$ $a=12.055\pm0.004$ Å |
| Composition: $\mathrm{di_{90}wo_{6.9}\ hem_{3.1}\ (=di_{90}\ andr_{10})}$ | | | | |
| xtl | 1380 | 2 h | glass | |
| xtl | 1375 | 2 h | cpx$_{ss}$+glass | rare cpx$_{ss}$ |
| glass | 1275 | 1 d | cpx$_{ss}$+glass | |
| xtl | 1270 | 2 d | cpx$_{ss}$+wo$_{ss}$+glass | traces of wo$_{ss}$ and glass |
| xtl | 1250 | 7 d | cpx$_{ss}$+wo$_{ss}$ | |
| glass | 1050 | 107 d | cpx$_{ss}$+wo$_{ss}$ | |
| Composition: $\mathrm{di_{80}wo_{13.7}hem_{6.3}(=di_{80}FTs_{20})}$ | | | | |
| xtl | 1365 | 2 h | glass | |
| xtl | 1360 | 2 h | cpx$_{ss}$+glass | small amounts of cpx$_{ss}$ |
| xtl | 1275 | 1 d | cpx$_{ss}$+glass | |
| xtl | 1250 | 2 d | cpx$_{ss}$+wo$_{ss}$+glass | wo$_{ss}$ in large amounts; glass in traces |
| xtl | 1200 | 7 d | cpx$_{ss}$+wo$_{ss}$ | |
| glass | 1050 | 60 d | cpx$_{ss}$+wo$_{ss}$ | |
| Composition: $\mathrm{di_{70}wo_{20.6}hem_{9.4}(=di_{70}\ andr_{30})}$ | | | | |
| xtl | 1345 | 2 h | glass | |
| xtl | 1340 | 2 h | cpx$_{ss}$+glass | traces of cpx$_{ss}$ |
| xtl | 1270 | 1 d | cpx$_{ss}$+wo$_{ss}$+glass | lots of cpx$_{ss}$; traces of wo$_{ss}$ |
| xtl | 1250 | 2 d | cpx$_{ss}$+wo$_{ss}$± glass | trace of glass |
| xtl | 1200 | 7 d | cpx$_{ss}$+wo$_{ss}$ | |
| glass | 1050 | 71 d | cpx$_{ss}$+wo$_{ss}$ | |
| Composition: $\mathrm{di_{55.6}wo_{30.4}hem_{14}(=di_{55.6}\ andr_{44.4})}$ | | | | |
| xtl | 1320 | 2 h | glass | |
| xtl | 1315 | 2 h | glass | one grain of cpx$_{ss}$ |
| xtl | 1310 | 2 h | cpx$_{ss}$+glass | small amounts of cpx$_{ss}$ |
| xtl | 1275 | 1 d | cpx$_{ss}$+glass | |
| xtl | 1265 | 1 d | cpx$_{ss}$+wo$_{ss}$+glass | very small amounts of wo$_{ss}$ |
| xtl | 1250 | 2 d | cpx$_{ss}$+wo$_{ss}$+glass | small amounts of glass |
| xtl | 1200 | 7 d | cpx$_{ss}$+wo$_{ss}$ | |
| xtl | 1175 | 14 d | cpx$_{ss}$+wo$_{ss}$+glass | very rare traces of hem |
| xtl | 1140 | 14 d | cpx$_{ss}$+wo$_{ss}$ | |
| xtl | 1130 | 14 d | cpx$_{ss}$+wo$_{ss}$+andr$_{ss}$ | |
| glass | 1050 | 78 d | cpx$_{ss}$+wo$_{ss}$+andr$_{ss}$ | andr$_{ss}$ $a=12.052\pm0.005$ Å |
| Composition: $\mathrm{di_{46.1}wo_{36.9}hem_{17}(=di_{46.1}andr_{53.9})}$ | | | | |
| glass | 1295 | 2 h | glass | |
| glass | 1290 | 2 h | cpx$_{ss}$+glass | |
| glass | 1270 | 7 d | cpx$_{ss}$+glass | |
| glass | 1200 | 7 d | cpx$_{ss}$+wo$_{ss}$+glass | traces of hem |
| glass | 1175 | 7 d | cpx$_{ss}$+wo$_{ss}$+hem +glass | traces of glass |
| Composition: $\mathrm{di_{36.5}wo_{43.5}hem_{20}(=di_{36.5}andr_{63.5})}$ | | | | |
| xtl | 1270 | 2 h | glass | |
| xtl | 1265 | 4 h | wo$_{ss}$+glass | small amounts of wo$_{ss}$ |
| xtl | 1260 | 6 h | cpx$_{ss}$+wo$_{ss}$+glass | small amounts of cpx$_{ss}$ |
| xtl | 1220 | 1 d | cpx$_{ss}$+wo$_{ss}$+glass | |
| xtl | 1210 | 1 d | cpx$_{ss}$+wo$_{ss}$+hem +glass | |
| xtl | 1160 | 14 d | cpx$_{ss}$+wo$_{ss}$+hem | |
| xtl | 1150 | 14 d | cpx$_{ss}$+wo$_{ss}$+andr$_{ss}$ | |
| glass | 1050 | 71 d | cpx$_{ss}$+wo$_{ss}$+andr$_{ss}$ | andr$_{ss}$ $a=12.056\pm0.004$ Å |
| Composition: $\mathrm{di_{28.3}wo_{49.1}hem_{22.6}(=di_{28.3}andr_{71.7})}$ | | | | |
| glass | 1275 | 2 h | glass | |
| glass | 1270 | 2 h | wo$_{ss}$+glass | lots of wo$_{ss}$ |
| glass | 1250 | 12 h | wo$_{ss}$+glass | |

TABLE 1—(*Continued*)

| Starting material$^a$ | T, °C | Time$^b$ | Products | Remarks |
|---|---|---|---|---|
| glass | 1240 | 12 h | wo$_{ss}$+cpx$_{ss}$+glass | |
| glass | 1235 | 1 d | wo$_{ss}$+cpx$_{ss}$+glass | lots of wo$_{ss}$ |
| glass | 1230 | 1 d | wo$_{ss}$+cpx$_{ss}$+hem +glass | |
| Composition: di$_{20}$wo$_{54.8}$hem$_{25.2}$(=di$_{20}$andr$_{80}$) | | | | |
| xtl | 1295 | 3 h | glass | |
| xtl | 1290 | 4 h | pwo+glass | |
| xtl | 1255 | 12 h | pwo+glass | |
| xtl | 1250 | 1 d | pwo+wo$_{ss}$+hem +glass | traces of hem |
| xtl | 1240 | 1 d | wo$_{ss}$+hem+glass | |
| xtl | 1225 | 7 d | wo$_{ss}$+cpx$_{ss}$+hem +glass | traces of cpx$_{ss}$ |
| xtl | 1200 | 14 d | cpx$_{ss}$+wo$_{ss}$+hem +glass | |
| xtl | 1160 | 14 d | cpx$_{ss}$+wo$_{ss}$+hem | |
| xtl | 1150 | 14 d | cpx$_{ss}$+wo$_{ss}$+andr$_{ss}$ | |
| xtl | 1135 | 14 d | cpx$_{ss}$+wo$_{ss}$+andr$_{ss}$ | andr$_{ss}$ $a=12.051\pm0.002$ Å |
| glass | 1050 | 57 d | cpx$_{ss}$+wo$_{ss}$+andr$_{ss}$ | andr$_{ss}$ $a=12.053\pm0.004$ Å |
| Composition: di$_{10}$wo$_{61.7}$hem$_{28.3}$(=di$_{10}$andr$_{90}$) | | | | |
| xtl | 1320 | 3 h | glass | |
| xtl | 1315 | 4 h | pwo+glass | rare pwo |
| xtl | 1275 | 12 h | pwo+glass | traces of hem |
| xtl | 1270 | 12 h | pwo+hem+glass | |
| xtl | 1230 | 2 d | pwo+hem+glass | traces of wo$_{ss}$ |
| xtl | 1210 | 3 d | wo$_{ss}$+hem+glass | glass in traces |
| xtl | 1200 | 14 d | cpx$_{ss}$+wo$_{ss}$+hem +glass | glass in traces |
| xtl | 1160 | 14 d | cpx$_{ss}$+wo$_{ss}$+hem | |
| xtl | 1145 | 14 d | cpx$_{ss}$+wo$_{ss}$+hem +andr$_{ss}$ | |
| xtl | 1135 | 14 d | cpx$_{ss}$+wo$_{ss}$+andr$_{ss}$ | andr$_{ss}$ $a=12.052\pm0.005$ Å |
| glass | 1050 | 99 d | cpx$_{ss}$+wo$_{ss}$+andr$_{ss}$ | andr$_{ss}$ $a=12.054\pm0.003$ Å |
| Composition: di$_5$wo$_{65.1}$hem$_{29.9}$(=di$_5$andr$_{95}$) | | | | |
| xtl | 1330 | 3 h | glass | |
| xtl | 1325 | 3 h | pwo+glass | lots of pwo |
| xtl | 1280 | 3 h | pwo+hem+glass | rare hem |
| xtl | 1210 | 3 d | pwo+hem+wo$_{ss}$ +glass | |
| xtl | 1200 | 14 d | pwo+hem+wo$_{ss}$ | |
| xtl | 1175 | 14 d | hem+wo$_{ss}$ | |
| xtl | 1160 | 14 d | hem+wo$_{ss}$ | traces of cpx$_{ss}$ |
| xtl | 1150 | 14 d | hem+wo$_{ss}$+cpx$_{ss}$ +andr$_{ss}$ | |
| xtl | 1145 | 14 d | hem+wo$_{ss}$+cpx$_{ss}$ +andr$_{ss}$ | traces of hem |
| xtl | 1140 | 14 d | wo$_{ss}$+cpx$_{ss}$+andr$_{ss}$ | |
| xtl | 1135 | 14 d | wo$_{ss}$+cpx$_{ss}$+andr$_{ss}$ | |
| xtl | 1050 | 125 d | wo$_{ss}$+cpx$_{ss}$+andr$_{ss}$ | andr$_{ss}$ $a=12.054\pm0.003$ Å |
| Composition: di$_0$wo$_{68.6}$hem$_{31.4}$(=di$_0$andr$_{100}$) | | | | |
| xtl | 1345 | 2 h | glass | |
| xtl | 1340 | 2 h | pwo+glass | pwo in moderate amounts |
| xtl | 1295 | 1 d | pwo+glass | glass in small amounts |
| xtl | 1290 | 1 d | pwo+hem | |
| xtl | 1160 | 28 d | pwo+hem | corroded andr$_{ss}$ in very small amounts |
| glass | 1160 | 28 d | pwo+hem | no andr$_{ss}$ |
| xtl | 1155 | 28 d | pwo+hem+andr$_{ss}$ | andr$_{ss}$ in traces; not corroded |
| glass | 1155 | 28 d | pwo+hem+andr$_{ss}$ | andr$_{ss}$ in traces; not corroded |
| xtl | 1150 | 14 d | pwo+hem+andr$_{ss}$ | andr$_{ss}$ $a_0=12.045\pm0.002$ Å |
| xtl | 1140 | 14 d | pwo+hem+andr$_{ss}$ | wo$_{ss}$ in traces |
| glass | 1140 | 14 d | pwo+hem+andr$_{ss}$ | hem in traces |
| xtl | 1135 | 14 d | andr$_{ss}$ | traces of wo$_{ss}$ and hem |
| glass | 1135 | 14 d | andr$_{ss}$ | very rare traces of wo$_{ss}$ and a few grains of hem |
| glass | 1135 | 56 d | andr$_{ss}$ | andr$_{ss}$ $a=12.053\pm0.003$ Å |
| glass | 1050 | 136 d | andr$_{ss}$ | andr$_{ss}$ $a=12.057\pm0.004$ Å; few grains of hem |
| glass | 900 | 42 d | andr$_{ss}$ | large amounts of wo$_{ss}$ and hem |
| glass | 800 | 42 d | wo$_{ss}$, hem and glass | no andr$_{ss}$ formed |
| Composition: di$_0$wo$_{73}$hem$_{27}$ | | | | |
| glass | 1315 | 2 d | pwo+glass | |
| glass | 1300 | 3 d | pwo+glass | |
| glass | 1250 | 3 d | pwo+hem | |
| glass | 1135 | 28 d | pwo+wo$_{ss}$+andr$_{ss}$ | wo$_{ss}$ in very rare amounts |
| glass | 1050 | 130 d | wo$_{ss}$+andr$_{ss}$ | andr$_{ss}$ $a=12.058\pm0.005$ Å |
| Composition: di$_{4.2}$wo$_{64.3}$hem$_{31.5}$(=andr$_{97}$kho$_3$) | | | | |
| xtl | 1155 | 14 d | wo$_{ss}$+hem | |
| xtl | 1135 | 28 d | cpx$_{ss}$+andr$_{ss}$ | cpx$_{ss}$ in very rare amounts; andr$_{ss}$ $a=12.051\pm0.003$ Å |
| glass | 1050 | 64 d | cpx$_{ss}$+andr$_{ss}$+hem | andr$_{ss}$ $a=12.055\pm0.004$ Å |
| Composition: di$_{14.1}$wo$_{54.1}$hem$_{31.8}$(=andr$_{90}$kho$_{10}$) | | | | |
| glass | 1270 | 2 h | glass | |
| glass | 1265 | 2 h | pwo+glass | |
| glass | 1255 | 3 h | pwo+hem+glass | hem in traces |
| xtl | 1240 | 1 d | pwo+hem+glass | |
| xtl | 1160 | 14 d | cpx$_{ss}$+wo$_{ss}$+hem | |
| xtl | 1145 | 14 d | cpx$_{ss}$+hem+andr$_{ss}$ | |
| xtl | 1135 | 14 d | cpx$_{ss}$+hem+andr$_{ss}$ | andr$_{ss}$ $a_0=12.051\pm0.003$ Å |
| glass | 1050 | 127 d | cpx$_{ss}$+hem+andr$_{ss}$ | andr$_{ss}$ $a_0=12.055\pm0.004$ Å |
| Composition: di$_{95}$wo$_0$hem$_5$ | | | | |
| xtl | 1292 | 1 d | cpx$_{ss}$ | |
| xtl | 1250 | 1 d | cpx$_{ss}$ | |
| xtl | 1200 | 3 d | cpx$_{ss}$ | |
| xtl | 1175 | 3 d | cpx$_{ss}$ | |
| xtl | 1155 | 7 d | cpx$_{ss}$ | hem in very rare traces; unit-cell parameters of cpx$_{ss}$ determined |
| xtl | 1100 | 7 d | cpx$_{ss}$+hem | very small amounts of hem |
| xtl | 1050 | 46 d | cpx$_{ss}$+hem | hem in very small amounts; unit-cell parameters of cpx$_{ss}$ determined |
| Composition: di$_{90}$wo$_0$hem$_{10}$ | | | | |
| xtl | 1292 | 1 d | cpx$_{ss}$+mt$_{ss}$+glass | |
| xtl | 1250 | 1 d | cpx$_{ss}$+hem | |
| xtl | 1150 | 7 d | cpx$_{ss}$+hem | |
| glass | 1050 | 61 d | cpx$_{ss}$+hem | |
| Composition: di$_{67.1}$wo$_{18.9}$hem$_{14}$ | | | | |
| xtl | 1325 | 2 h | glass | |
| xtl | 1320 | 2 h | cpx$_{ss}$+glass | |
| xtl | 1250 | 1 d | cpx$_{ss}$+glass | |
| xtl | 1175 | 7 d | cpx$_{ss}$+wo$_{ss}$ | |
| xtl | 1150 | 7 d | cpx$_{ss}$+wo$_{ss}$ | |
| glass | 1050 | 60 d | cpx$_{ss}$+wo$_{ss}$ | traces of andr$_{ss}$ |
| Composition: di$_{70}$wo$_{15}$hem$_{15}$ | | | | |
| xtl | 1250 | 3 d | cpx$_{ss}$+glass | |
| xtl | 1175 | 7 d | cpx$_{ss}$ | traces of glass |
| xtl | 1155 | 7 d | cpx$_{ss}$ | unit-cell parameters of cpx$_{ss}$ determined |
| glass | 1050 | 61 d | cpx$_{ss}$ | unit-cell parameters of cpx$_{ss}$ determined |
| Composition: di$_{63.2}$wo$_{18.1}$hem$_{18.7}$ | | | | |
| xtl | 1250 | 3 d | cpx$_{ss}$+glass | |
| xtl | 1175 | 7 d | cpx$_{ss}$+glass | |
| xtl | 1155 | 7 d | cpx$_{ss}$ | few grains of hem; unit-cell parameters of cpx$_{ss}$ determined |
| xtl | 1050 | 10 d | cpx$_{ss}$+hem+andr$_{ss}$ | |

[a] xtl = crystalline material prepared at 1050°C; products as listed in table for that temperature; abbreviations of the phases present are given in the text.

[b] h = hours; d = days.

of the phases therefore cannot be expressed solely in terms of di, wo, and hem, and the system should properly be treated as quaternary. However, the amount of ferrous iron present in the runs crystallized at 1050° and 1155°C (Table 2) is less than 5 percent of the total iron (expressed as $Fe_2O_3$). Hence these compositions lie very close to the di-wo-hem plane. Starting mixtures quenched from a temperature of 1500°C contain 10 to 20 percent FeO in the liquid. Isopleths of approximately constant $FeO/Fe_2O_3$ (total) were constructed in the plane di-wo-hem from the analytical data available for temperatures of 1050°, 1155°, and 1500°C (Fig. 3). It can be seen that the amount of ferrous iron decreases with increase of both the andradite component and the ferri-Tschermak's molecule.

TABLE 2. FeO CONTENTS OF CHEMICALLY ANALYZED COMPOSITIONS ON THE JOIN DI-WO-HEM AT TEMPERATURES OF 1050°, 1155°, AND 1500°C

| Composition | | | % FeO at | | | $FeO/Fe_2O_3$ (total Fe) at | | |
|---|---|---|---|---|---|---|---|---|
| di | wo | hem (= $Fe_2O_3$) | 1050° | 1155° | 1500° | 1050° | 1155° | 1500° |
| 90 | 4.2 | 5.79 | 0.28 | | 0.90 | 0.049 | | 0.155 |
| 80 | 8.4 | 11.58 | .30 | 0.53 | 1.92 | .026 | 0.046 | .166 |
| 75 | 10.5 | 14.47 | .30 | 0.74 | 2.40 | .021 | .051 | .166 |
| 68.9 | 13.1 | 18.00 | .35 | 1.15 | 2.80 | .019 | .064 | .156 |
| 65 | 14.7 | 20.27 | .25 | | 2.60 | .012 | | .128 |
| 59.3 | 17.2 | 23.50 | .30 | | 2.16 | .013 | | .134 |
| 55.5 | 19 | 25.50 | | | 3.40 | | | .133 |
| 51.6 | 20.4 | 28.00 | .27 | | 3.75 | .010 | | .134 |
| 43 | 34 | 33.00 | .32 | | 4.50 | .010 | | .136 |
| 30 | 29.5 | 40.53 | .22 | | | .005 | | |
| 20 | 33.7 | 46.32 | .16 | | | .003 | | |
| 10 | 37.9 | 52.11 | .10 | | 5.20 | .002 | | .099 |
| 0 | 42.1 | 57.90 | .10 | | | .002 | | |
| 90 | 6.9 | 3.14 | .28 | | 0.65 | .089 | | .205 |
| 80 | 13.7 | 6.29 | .34 | | 0.84 | .054 | | .133 |
| 70 | 20.6 | 9.43 | .20 | | 1.50 | .021 | | .159 |
| 55.6 | 30.4 | 14.00 | .21 | | 1.60 | .015 | | .114 |
| 46.1 | 36.9 | 17.00 | | | 2.40 | | | .141 |
| 36.5 | 43.5 | 20.00 | .18 | | | .009 | | |
| 28.3 | 49.1 | 22.57 | | | 2.56 | | | .113 |
| 20 | 54.8 | 25.15 | .20 | | 2.96 | .008 | | .118 |
| 10 | 61.7 | 28.30 | .14 | | 3.00 | .005 | | .106 |
| 5 | 65.1 | 29.87 | .13 | | | .004 | | |
| 0 | 68.6 | 31.44 | .15 | | | .005 | | |
| 4.2 | 64.3 | 31.54 | .20 | | 3.40 | .006 | | .108 |
| 14.1 | 54.1 | 31.76 | .15 | | 3.50 | .005 | | .110 |
| 95 | 0 | 5.00 | .24 | 0.40 | 1.00 | .048 | .080 | .200 |
| 90 | 0 | 10.00 | | | 2.10 | | | .210 |
| 67.1 | 18.9 | 14.00 | .30 | | 1.76 | .021 | | .126 |
| 70 | 15 | 15.00 | .26 | | 2.50 | .017 | | .166 |
| 63.2 | 18.1 | 18.75 | | 0.58 | | | .031 | |

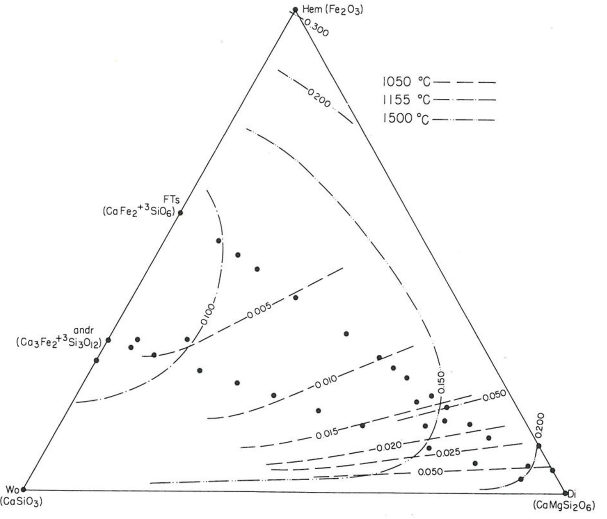

FIG. 3. The diopside-wollastonite-hematite plane with curves of approximately constant $FeO/Fe_2O_3$ ratios at various temperatures. The ratios give an estimate of the departure of a mixture from ideal Di-Wo-Hem compositions within the Di-Wo-Hem-Mt tetrahedron and in partial measure the degree of deviation from ternary relationships at temperatures of 1050°, 1155°, and 1500°C.

*The join diopside—ferri-Tschermak's molecule.* The stable phases crystallizing at atmospheric pressure on the join di-FTs (Fig. 4) are clinopyroxene solid solution ($cpx_{ss}$), wollastonite solid solution ($wo_{ss}$), pseudowollastonite (pwo), andradite solid solution ($andr_{ss}$), magnetite solid solution ($mt_{ss}$), and hematite (hem). $Magnetite_{ss}$ is stable only in the presence of a liquid, and $andr_{ss}$, only in the subsolidus region.

The maximum stable solid solution of ferri-Tschermak's molecule in diopside is greater than 31.1 and less than 35.0 weight percent and is believed to be close to 33 weight percent at 1175°C. The extent of solid solution was estimated from unit-cell parameters of pyroxenes along the join di-FTs that had been held for several days at 1050° or

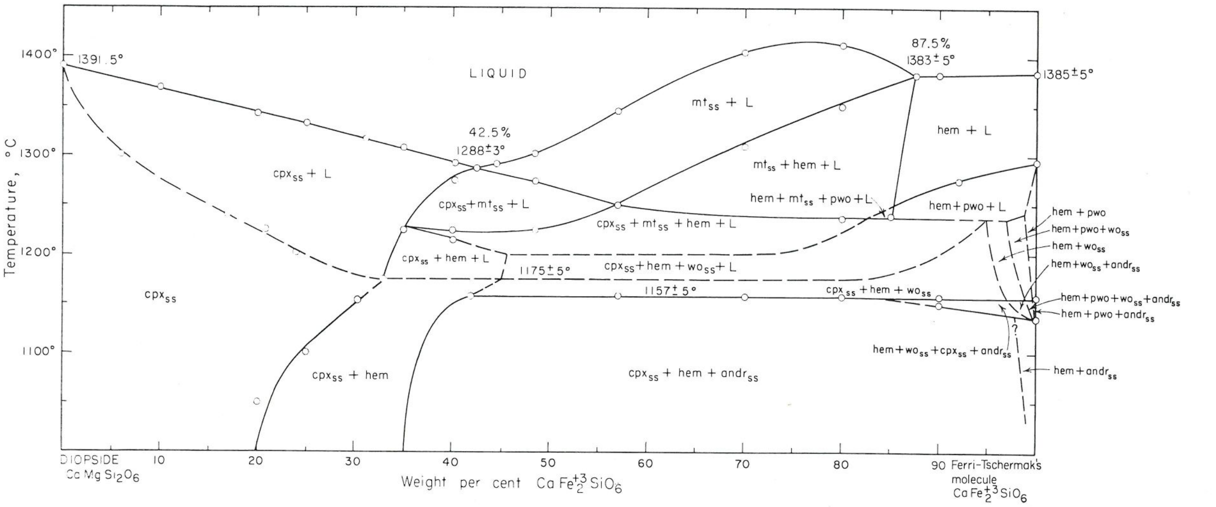

FIG. 4. Temperature versus composition plot of data obtained on the join diopside—ferri-Tschermak's molecule at 1 atmosphere. Abbreviations for phases encountered: $cpx_{ss}$, clinopyroxene solid solution; $mt_{ss}$, magnetite solid solution; hem, hematite; pwo, pseudowollastonite; $wo_{ss}$, wollastonite solid solution; and $andr_{ss}$, andradite solid solution.

TABLE 3. UNIT-CELL PARAMETERS OF DIOPSIDE AND FERRI-DIOPSIDE SOLID SOLUTION

| Composition | Crystallized at T (°C) | $a$, Å[b] | $b$, Å[b] | $c$, Å[b] | $\beta$, degrees[b] | $V$, Å$^3$[b] |
|---|---|---|---|---|---|---|
| diopside (Clark *et al.*, 1962) | subsolidus | 9.745(1) | 8.925(1) | 5.248(1) | 105.87(1) | 439.08(7) |
| $Di_{90}FTs_{10}$ | 1050 | 9.762(3) | 8.928(3) | 5.259(2) | 105.84(3) | 440.99(21) |
| | 1155 | 9.761(2) | 8.928(1) | 5.269(2) | 105.87(1) | 441.57(18) |
| $Di_{80}FTs_{20}$ | 1050 | 9.773(2) | 8.916(2) | 5.286(2) | 105.90(2) | 443.47(14) |
| | 1155 | 9.776(3) | 8.922(2) | 5.276(3) | 105.90(3) | 442.58(39) |
| $Di_{75}FTs_{25}$ | 1155 | 9.781(3) | 8.915(2) | 5.293(2) | 105.88(2) | 443.94(28) |
| $Di_{68.9}FTs_{31.1}$ | 1155 | 9.788(4) | 8.911(2) | 5.308(2) | 105.90(3) | 445.24(29) |
| $Di_{70}Wol_{4.1}FTs_{25.9}$ | 1050 | 9.789(2) | 8.920(2) | 5.298(1) | 105.86(2) | 445.01(13) |
| $Di_{69}Wo_{5}FTs_{26}$[a] | 1050 | 9.80(1) | 8.91(1) | 5.31(1) | 105.9(1) | 445.7(8) |
| $Di_{63.2}Wo'_{4.5}FTs_{32.3}$ | 1155 | 9.801(3) | 8.912(3) | 5.319(4) | 105.87(3) | 446.85(26) |
| $Di_{95}Hem_{5}$ | 1050 | 9.753(3) | 8.929(2) | 5.260(2) | 105.97(3) | 440.36(16) |
| | 1155 | 9.758(2) | 8.928(2) | 5.263(1) | 105.92(2) | 440.96(10) |

[a] Estimated clinopyroxene composition. Crystallized from a $DI_{59.3}WO_{17.2}HEM_{23.5}$ bulk composition in the $cpx_{ss}$+hem+$andr_{ss}$ phase assemblage.

[b] Plus-and-Minus error in last place(s) given in parentheses.

1155°C. Least-squares refinement of data obtained from powder X-ray diffraction charts (CuK$\alpha$; $\lambda = 1.5418$ Å) was carried out with a program written by Charles W. Burnham at the Geophysical Laboratory for the IBM 7094 digital computer. The reflections measured were (150), (510), (132), (240), (041), (421), (331), (330), $(31\bar{1})$, $(22\bar{1})$, (202), (131), (311), (310), (221), (220), and (021) using silicon as an internal standard. Table 3 and Figure 5 show the results, together with data obtained by Coleman (1962) on synthetic pyroxenes containing up to 10 mole percent FTs. There is a substantial increase of $a$, $c$, and $V$, but a decrease of $b$ from diopside to $di_{68.9}$ $FTs_{31.1}$. The angle $\beta$ remains essentially constant. Coleman's data reveal the same tendencies in cell constants; however, they show greater variance than the data obtained in the present study.

The substitution of $Fe^{3+}Fe^{3+}$ for MgSi within the range of stable solid solution along the join di-FTs at 1155°C expands the cell volume $V$ by about 14 percent.[1] Comparison of the average tetrahedral distances of Si-O (1.61 Å; taken from *International Tables for X-Ray Crystallography*, Vol. 3, 1962) and $Fe^{3+}$-O (1.86 Å) and the octahedral distances of Mg-O (2.07 Å) and $Fe^{3+}$-O (2.01 Å) shows the more marked difference for tetrahedral substitution by $Fe^{3+}$. In short, substitution of $Fe^{3+}$ considerably expands the tetrahedra and slightly shrinks the octahedra. The substitution of $Fe^{3+}$ for Mg within the octahedra results in a minor decrease of $b$, whereas the expansion of the tetrahedra is revealed not only in $c$ but also in $a$. The increase of $c$ is caused only by the substitution of $Fe^{3+}$ for Si. On the other hand, the change of $a$ is produced by a contraction of the octahedra as well, and the expansion of the tetrahedra in this direction is very much larger than the contraction of the octahedra because two expanded $(Si,Fe^{3+})_2O_6$ chains of the diopside structure are involved. The FeO contents in the range of the stable solid solution are small (Table 2) and should cause no measurable change in the cell dimension.

The angular separation of certain pairs of reflections can be used to determine the composition of ferri-diopside solid solution along the join di-FTs, as well as in certain portions of the di-wo-hem plane. The most sensitive angular separation is that of $2\theta(240)$–$2\theta(041)$; the intensity of these reflections is low, however, and the technique cannot be applied in polyphase assemblages. Another angular separation, $2\theta(22\bar{1})$–$2\theta(202)$, is useful, except in the range $di_{100}FTs_0$ to $di_{90}FTs_{10}$, where the determinative curve passes through a minimum and where the hematite content is higher. The $(11\bar{2}0)$ reflection of hematite at 35.5° $2\theta$ coincides with the (221) reflection of the ferri-diopside solid solution (Fig. 6).

The $clinopyroxene_{ss}$ formed at solidus temperatures in compositions between 20 percent (at 1000°C) and 33 percent (at 1175°C) FTs breaks down with the cooling to a $clinopyroxene_{ss}$ + hematite. These particular clinopyroxene solid solutions must lie off the join di-FTs in the more wollastonite-rich part of the di-wo-hem plane, as can be seen from an inspection of the isothermal sections at 1050°, 1137°, and 1157°C (Figs. 9, 10, and 11). The $clinopyroxene_{ss}$ in coexistence with hematite was examined by X-rays with the reflection pairs described above. The values are slightly different from those extrapolated from clinopyroxenes that lie directly on the join without hematite.

The $cpx_{ss}$ + hem assemblage is replaced by $cpx_{ss}$ + hem + $andr_{ss}$ at compositions greater than 35 to 44 weight percent at 1000° and 1175°C, respectively. The clinopy-

---

[1] The increase in cell volume suggests that the end-member composition of the ferri-Tschermak's molecule is not likely to crystallize as a pyroxene even at high pressures. Preliminary runs were carried out on the pure FTs composition at 20 kb and 1300°C in solid-media pressure apparatus through the courtesy of Professor W. Schreyer, and the phases obtained were $andradite_{ss}$ + hematite and small amounts of magnetite.

roxene$_{ss}$ occurring in the three-phase assemblage cannot lie on the join di-FTs. On the basis of cell determinations and inspection of the corresponding isothermal sections, the pyroxene compositions were found to be $di_{69}wo_{16}hem_{15}$ at 1050°C, $di_{66}wo_{17}hem_{17}$ at 1137°C, and $di_{62}wo_{19}hem_{19}$ at 1157°C. These pyroxene solid solutions may also be expressed as $di_{69}wo_{5}FTs_{26}$, $di_{66}wo_{5}FTs_{29}$, and $di_{62}wo_{5}FTs_{33}$; or as $di_{69}FTs_{20}andr_{11}$, $di_{66}FTs_{24}andr_{19}$, and $di_{62}FTs_{27}andr_{11}$. That is, either wollastonite or andradite may be considered as solid solutions in those diopsides in addition to the ferri-Tschermak's molecule. Unit-cell parameters were measured for clinopyroxenes with the compositions $di_{70}wo_{4.1}FTs_{25.9}$ ($= di_{70}FTs_{21.1}andr_{8.9}$), $di_{69}wo_{5}FTs_{26}$ ($= di_{69}FTs_{20}andr_{11}$), and $di_{63.2}wo_{4.5}FTs_{32.3}$ ($= di_{63.2}FTs_{27.2}andr_{9.6}$). The expansion of the unit cells of these particular clinopyroxenes appears to be slightly favored if Mg is replaced by Ca in addition to the substitution of $Fe^{3+}Fe^{3+}$ for MgSi (Table 3).

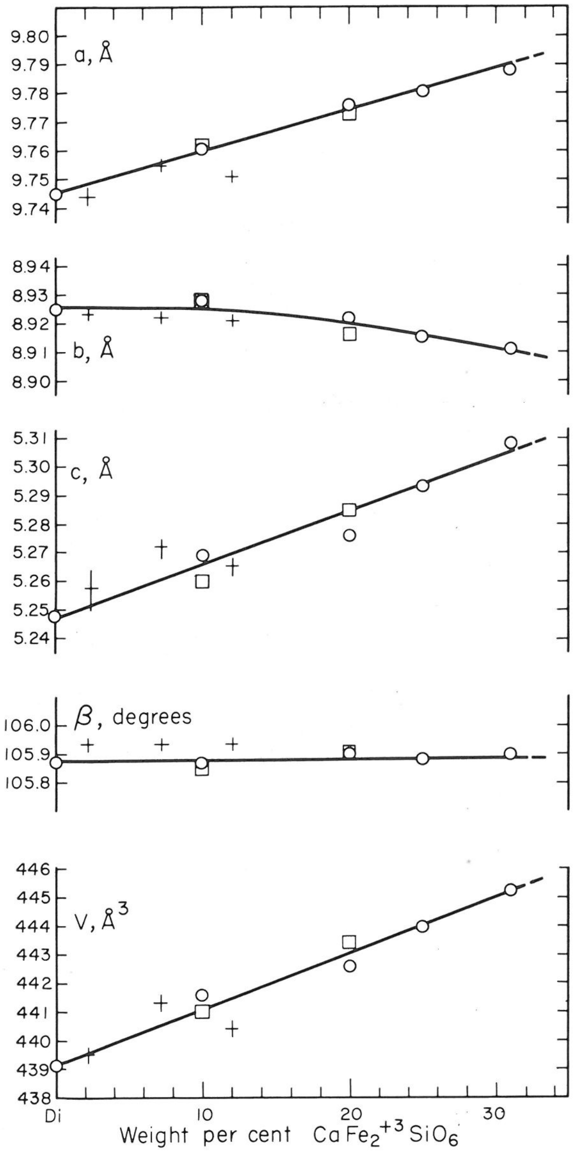

FIG. 5. Unit-cell parameters within the range of stable solid solution along the join diopside—ferri-Tschermak's molecule. The clinopyroxene solid solutions were crystallized at 1050°C (squares) and 1155°C (circles), respectively. Crosses represent Coleman's data (1962).

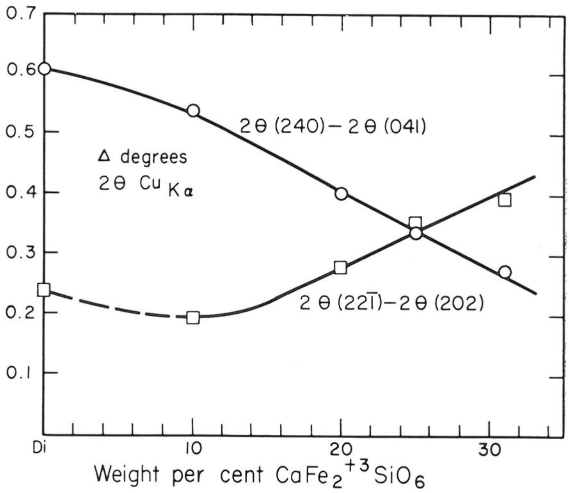

FIG. 6. Change of angular separations of $2\Theta(240)-2\Theta(041)$ and $2\theta(221)-2\theta(202)$ within the range of stable solid solution along the join diopside—ferri-Tschermak's molecule.

The coexisting garnet in the three-phase assemblage cpx$_{ss}$ + hem + andr$_{ss}$ is almost pure andradite and has a cell edge similar to that of the end member on the join diopside-andradite (Fig. 7), because the very limited replacement of Ca by Mg does not effect a measurable change in *a*. At temperatures above 1157°C, cpx$_{ss}$ + hem + andr$_{ss}$ is no longer stable and is replaced by cpx$_{ss}$ + hem + wo$_{ss}$. Wollastonite coexisting with diopside on the join $CaMgSi_2O_6$-$CaSiO_3$ has a composition $wo_{93}di_7$ at that temperature according to Schairer and Bowen (1942).

The liquidus phases on the join diopside—ferri-Tschermak's molecule are clinopyroxene, magnetite, and hematite. With powder X-ray diffraction and electron microprobe techniques it is possible to define the composition of the primary phases that crystallize near liquidus temperatures. Primary hematite contains traces of Mg and Ca, and even the ferrous iron content, which cannot as yet be demonstrated by electron microprobe analysis, must be low. Phillips and Muan (1960) reported the very limited solid solution of magnetite in hematite of 1 percent at about 1400°C in air. The primary magnetites consist of solid solutions of $Fe^{2+}Fe_2^{3+}O_4$ (magnetite) and $MgFe_2^{3+}O_4$ (magnesioferrite), including a small amount of $CaFe_2^{3+}O_4$. The total iron determined as $Fe_2O_3$ by electron microprobe analyses was partitioned into $Fe^{3+}$ and $Fe^{2+}$ as required for electrostatic balance in the magnetite formula. Bulk compositions $di_{51.6}FTs_{48.4}$, $di_{43}FTs_{57}$, and $di_{30}FTs_{70}$ form magnetite solid solutions + liquid and the magnetite has

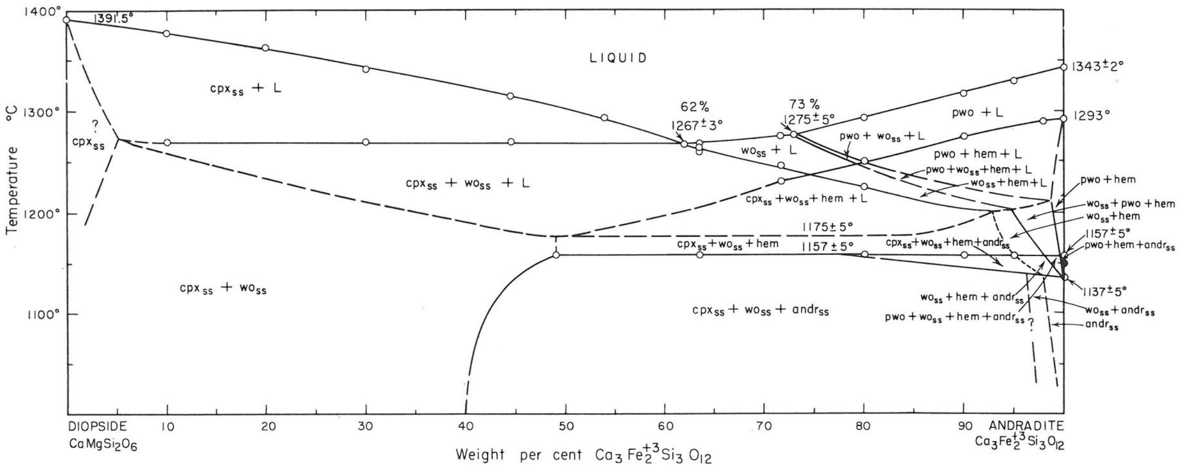

FIG. 7. Temperature versus composition plot of data obtained on the join diopside-andradite at 1 atmosphere. Abbreviations as in Figure 4.

the composition $(Mg_{0.52}Ca_{0.04}Fe_{2.44})O_4$ at 1290°C, $(Mg_{0.31}Ca_{0.03}Fe_{2.66})O_4$ at 1300°C, $(Mg_{0.26}Ca_{0.03}Fe_{2,71})O_4$ at 1325°C, and $(Mg_{0.29}Ca_{0.02}Fe_{2.69})O_4$ at 1380°C. It can be seen that the Mg content of the magnetite$_{ss}$ increases with increase of the $CaMgSi_2O_6$ component in the bulk composition. This is due to the relative relationship of the solid solution series magnesioferrite-magnetite and diopside—ferri-Tschermak's molecule in the $CaO$-$MgO$-$Fe_2O_3$—$FeO$-$SiO_2$ system. The two series are essentially parallel, and tie lines from magnetite$_{ss}$ to liquid intersect the join di-FTs at a high angle on the di-wo-hem plane. Therefore, an increase of Mg in the bulk composition will increase the Mg content in the magnetite$_{ss}$ as well.

Primary clinopyroxene$_{ss}$ coexisting with liquid has a composition of about di$_{94}$FTs$_6$ at 1300°C. The liquid leaves the join di-FTs at a temperature of 1288° ± 3°C and moves to the region of the di-wo-hem plane poorer in total iron than that join. At temperatures between 1288° and 1175°C the composition of the primary clinopyroxenes, therefore, being slightly enriched in ferric iron, must lie off the join di-FTs, as one can see by an inspection of the isothermal (pseudoternary) section at 1250°C (Fig. 12). The divergence in composition from ideal di-FTs clinopyroxene solid solutions is trifling. The compositions of the primary clinopyroxenes were determined by the angular separation of $2\theta(240)$-$2\theta(041)$ in order to fix the approximate location of the solidus in the diopside-rich part of the di-FTs join (Fig. 4). The compositions were found to be di$_{83}$FTs$_{17}$ at 1240°C, di$_{79}$FTs$_{21}$ at 1225°C, di$_{76}$FTs$_{24}$ at 1200°C.

*The join diopside-andradite.* The stable phases crystallizing on the join diopside-andradite (Fig. 7) are clinopyroxene$_{ss}$, wollastonite$_{ss}$, pseudowollastonite, hematite, and andradite$_{ss}$. The phases present in the diopside-rich part of the diagram are clinopyroxene$_{ss}$ and wollastonite$_{ss}$. Immediately below the solidus near pure diopside some solid solution of andradite in diopside has been assumed but not demonstrated with the data at hand. On the basis of cell parameters, the clinopyroxene$_{ss}$ must lie between the joins di-FTs and di-andr within the di-wo-hem plane (Figs. 9, 10, and 11). The assemblage cpx$_{ss}$ + wo$_{ss}$ in the region from andr$_{40}$ to andr$_{49}$ is replaced at lower temperatures by cpx$_{ss}$ + wo$_{ss}$ + andr$_{ss}$. Andr$_{ss}$ + wo$_{ss}$, and andr$_{ss}$, are the stable phases at compositions greater than andr$_{97}$ and andr$_{99}$, respectively, at the lowest temperatures investigated.

At temperatures above 1157°C andradite is not a stable phase, and there is a change in the mineral assemblages to pseudowollastonite + hematite, pseudowollastonite + wollastonite$_{ss}$ + hematite, wollastonite$_{ss}$ + hematite, and hematite + clinopyroxene$_{ss}$ + wollastonite$_{ss}$. As in the di-FTs join, there is a small field in which an andradite solid solution is stable in the presence of hematite and either wo$_{ss}$ or pwo, or both, from 1137° to 1157°C.

Garnet crystallizing from the andradite bulk composition has a unit-cell parameter of 12.057 ± 0.004 Å at 1050°C, 12.053 ± 0.003 Å at 1135°C, and 12.045 ± 0.002 Å at 1150°C (Table 4), determined with the use of reflections (642), (640), (611), (521), (510), (422), (420), and (400) with silicon as an internal standard. The shrinkage of the unit-cell parameters from 12.057 to 12.045 is probably caused by ubiquitous ferrous iron forming a skiagite molecule of $Fe_3{}^{2+}Fe_2{}^{3+}Si_3O_{12}$ composition, in which $Fe^{2+}$ substitutes for Ca. The amount of ferrous iron, determined by the methods of Shapiro and Brannock (1962), is 0.15 percent in andradite stable at 1050°C and has increased to 0.25 percent in andradite formed at 1135°C. Above 1137°C ± 5°C the garnet starts to decompose, and because pseudowollastonite and hematite can incorporate only small amounts of the ferrous iron present in the mixture (0.31 percent FeO at 1150°C), the remainder enters the andradite structure, resulting in markedly different cell sizes of garnet stable above and below 1137°C. Andradite

TABLE 4. UNIT-CELL PARAMETER OF ANDRADITES CRYSTALLIZED ON THE JOIN DI-WO-HEM

| Phase assemblage | $a$, Å | Crystallized at T (°C) | Remarks |
|---|---|---|---|
| andr$_{ss}$ | 12.057±0.004 | 1050[a] | Crystallized from a glass of andradite bulk composition, containing 0.15% FeO after treatment. |
| andr$_{ss}$ | 12.053±0.003 | 1135 | Crystallized from a glass of andradite bulk composition containing 0.25% FeO after treatment. |
| andr$_{ss}$+pwo+hem | 12.045±0.002 | 1150 | Breakdown assemblage from the andradite bulk composition; the mixture contains 0.31% FeO after treatment. |
| andr$_{ss}$+hem | 12.055±0.004 | 1050 | Andradite crystallized from the ferri-Tschermak's molecule bulk composition; the mixture contains 0.10% FeO after treatment. |
| andr$_{ss}$+hem | 12.052±0.004 | 1135 | Andradite crystallized from the ferri-Tschermak's molecule bulk composition. |
| andr$_{ss}$+wo$_{ss}$ | 12.058±0.005 | 1050 | Andradite from the wo$_{73}$hem$_{27}$ bulk composition. |
| andr$_{ss}$+hem+cpx$_{ss}$ | 12.054±0.002 | 1050 | Average of 6 andradites crystallizing in that phase assemblage; khoharite in andradite about 1%; the mixtures contain 0.10 to 0.32% FeO after treatment. |
| andr$_{ss}$+hem+cpx$_{ss}$ and andr$_{ss}$+cpx$_{ss}$ | 12.052±0.002 | 1135 | Average of 5 andradites crystallizing in that phase assemblage; khoharite in andradite about 2%. |
| andr$_{ss}$+wo$_{ss}$+cpx$_{ss}$ | 12.054±0.002 | 1050 | Average of 5 andradites crystallizing in that phase assemblage; khoharite in andradite about 1%; the mixtures contain 0.13 to 0.21% FeO after treatment. |
| andr$_{ss}$+wo$_{ss}$+cpx$_{ss}$ | 12.052±0.001 | 1135 | Average of 2 andradites crystallizing in that phase assemblage; khoharite in andradite about 2%. |

[a] Duration of treatment listed in Table 1.

itself breaks down completely to pwo + hem at 1157° ± 5°C.

The range of substitution of Mg for Ca in andradite and its effect on the cell dimensions were investigated by studying two compositions on the join andradite-khoharite (the theoretical garnet of $Mg_3Fe_2^{3+}Si_3O_{12}$ composition on the join enstatite-hematite if the di-wo-hem plane were extended to $MgSiO_3$ composition). There is very limited solid solution of khoharite in andradite: about 1 percent at 1050°C and 2 percent at 1137°C. The substitution does not cause a measurable change in the cell edge of the garnet; however, the average $a$ of andradites crystallizing in the andr$_{ss}$ + hem + cpx$_{ss}$, andr$_{ss}$ + cpx$_{ss}$, and andr$_{ss}$ + wo$_{ss}$ + cpx$_{ss}$ assemblages is slightly smaller compared with those crystallizing on the join wollastonite-hematite (Table 4).

The unit-cell parameter of the pure andradite end member obtained in this study is higher than those reported (see Table 5) by Skinner (1956) and Ernst (1966) and lower than those given by Swanson *et al.* (1960), Geller *et al.* (1964), and Ito and Frondel (1967). Natural garnet of almost pure andradite composition from Val Malenco near Sondria, northern Italy, has a unit-cell parameter of 12.061 Å. Its structure has been determined recently by Quareni and Pieri (1966). The reasons for the differences in cell size are not as yet well understood; however, the crystallizing techniques and conditions of formation will have considerable influence. The effects of water (hydrogarnet), oxidation state (skiagite), and temperature on cell dimension are evident. The conditions of formation of the garnets described in the previous studies are not sufficiently well defined for a valid comparison of cell dimensions. Evidence for a cell size smaller than that proposed by Geller (1967) may be deduced from andradite solid solutions crystallizing on the join andradite–Ti-garnet (Huckenholz, 1969). The cell parameter of the andr$_{46}$Ti-gar$_{54}$ end member stable at 1100°C is 12.250 Å. The decrease of the unit-cell parameter is 0.038 Å per 10 weight percent andradite, and cell sizes indicated for pure andradite are smaller than that given by Geller (1967).

TABLE 5. UNIT-CELL PARAMETER OF ANDRADITES FROM PREVIOUS STUDIES

| Reference | $a$, Å | Remarks |
|---|---|---|
| Skinner (1956) | 12.048 | Synthesized in solid-media pressure apparatus by the Norton Company from oxide mixtures of andradite bulk composition at unstated temperature and pressure. $n=1.887$. |
| Swanson *et al.* (1960, p. 22) | 12.059 | Synthesized hydrothermally at 850° and 20,000 psi in a cold-seal pressure vessel. Prepared from a gel of nitrates of ferric iron and calcium and ethyl orthosilicate. $n=1.887$. |
| Geller *et al.* (1964) | 12.067 | Synthesized dry from oxides at 1 atmosphere by means of a lithium molybdate flux (W. Bonner, personal communication, 1969). |
| Ernst (1966) | 12.040±0.010 | Average of 4 andradites synthesized hydrothermally from a ferrotremolite bulk composition; the oxygen fugacities were defined by hematite-magnetite and hausmannite-manganosite buffers. Detailed data are:<br>$T$, °C  $P$, bars  log $f_{O_2}$  Time, hr  $a$, Å<br>620  500  −13.7  316  12.036<br>594  3010  −14.5  362  12.040<br>514  2990  −17.5  2423  12.040<br>548  1990  −18.2  2420  12.045 |
| Ito and Frondel (1967) | 12.06 ±0.01 | Synthesized from a gel of andradite bulk composition at 1050°C for about 7 hours. |
| Quareni and de Pieri (1966) | 12.061 | Natural specimen of almost pure andradite composition from Val Malenco near Sondria, northern Italy. |

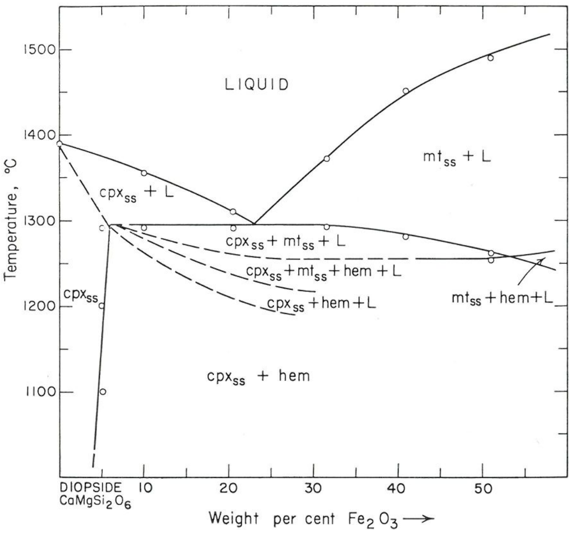

FIG. 8. Temperature versus composition plot of data obtained from Presnall (1966) and in this study on the join diopside-hematite at 1 atmosphere. Abbreviations as in Figure 4.

←

---

*The join diopside-hematite.* Presnall (1966) determined the liquidus relationships for this join, and Segnit (1953) studied the incorporation of ferric iron in diopside within the subsolidus region. Segnit reported that a maximum of 10 weight percent $Fe_2O_3$ was present in the diopside; unfortunately, no temperature data are given. With Presnall's liquidus data and the data obtained from quenching experiments in this study, it can be seen in Figure 8 that the solid solution of hematite in diopside is very limited. It is about 5 weight percent at 1050° and increases to a maximum of about 7 weight percent at 1292° ± 5°C. The sub-

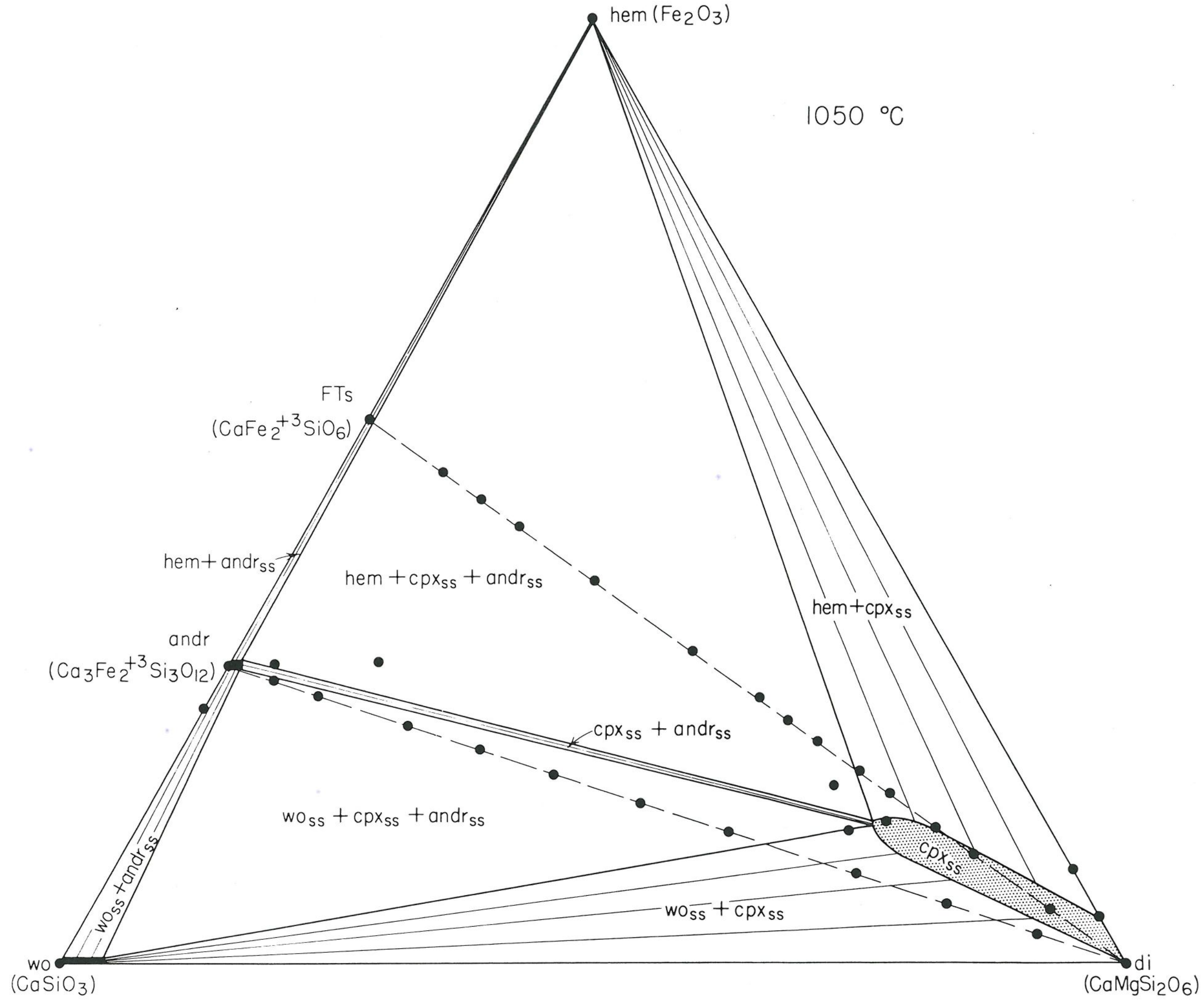

FIG. 9. Isothermal section of the diopside-wollastonite-hematite join at 1050°C.

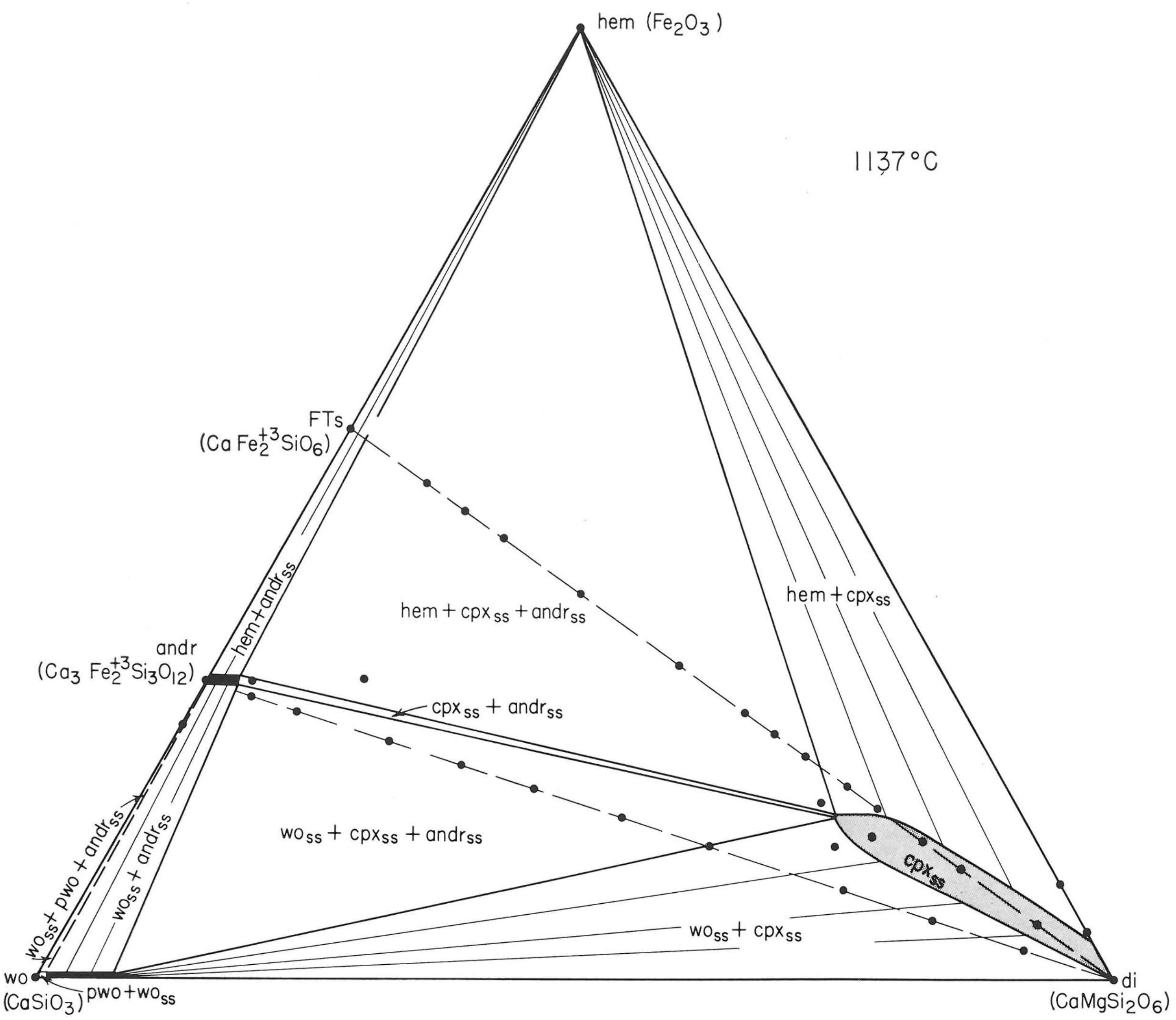

FIG. 10. Isothermal section of the diopside-wollastonite-hematite join at 1137°C.

stitution along the join diopside-hematite can be expressed in two parts as $2Fe^{3+}$ for MgSi, demonstrated on the join diopside—ferri-Tschermak's molecule, as well as $2Fe^{3+}$ for CaSi. The unit-cell parameters were determined for the $di_{95}hem_5$ composition (Table 3). The data for *a, b, c,* and *V* correspond very closely to those obtained on the join di-FTs. The angle $\beta$, however, appears to be slightly increased, probably owing to the occupation of Ca by $Fe^{3+}$ in the diopside structure.

## ISOTHERMAL SECTIONS AT 1050°, 1137°, 1158°, AND 1250°C OF THE di-wo-hem PLANE

The results of the thermal studies outlined previously are shown graphically in four isothermal sections. The 1050°, 1137°, 1158°, and 1250°C sections have been chosen to illustrate the change in the phase relationships and the variations of clinopyroxene and garnet solid solutions.

*Isothermal section at 1050°C (Fig. 9).* The stable phases at 1050°C are $cpx_{ss}$, hem, $wo_{ss}$, and $andr_{ss}$. In the di-rich portion of the plane, $cpx_{ss}$ + hem as well as $cpx_{ss}$ + $wo_{ss}$ coexist. The phase assemblages in the wo-rich portion are $wo_{ss}$ + $andr_{ss}$ and hem + $andr_{ss}$. The largest range of compositions is represented by the assemblage hem + $cpx_{ss}$ + $andr_{ss}$. It is separated from the $wo_{ss}$ + $cpx_{ss}$ + $andr_{ss}$ assemblage by a narrow two-phase field of $cpx_{ss}$ + $andr_{ss}$.

*Isothermal section at 1137°C (Fig. 10).* In the isothermal section at 1137°C a small field of pwo + $wo_{ss}$ + $andr_{ss}$ appears on the wo-andr join in addition to those phase assemblages encountered in the section at 1050°C. The range of stable solid solution of clinopyroxene has expanded to $di_{66}wo_{17}hem_{17}$; the khoharite component in the andradite$_{ss}$ has increased to about 2 percent.

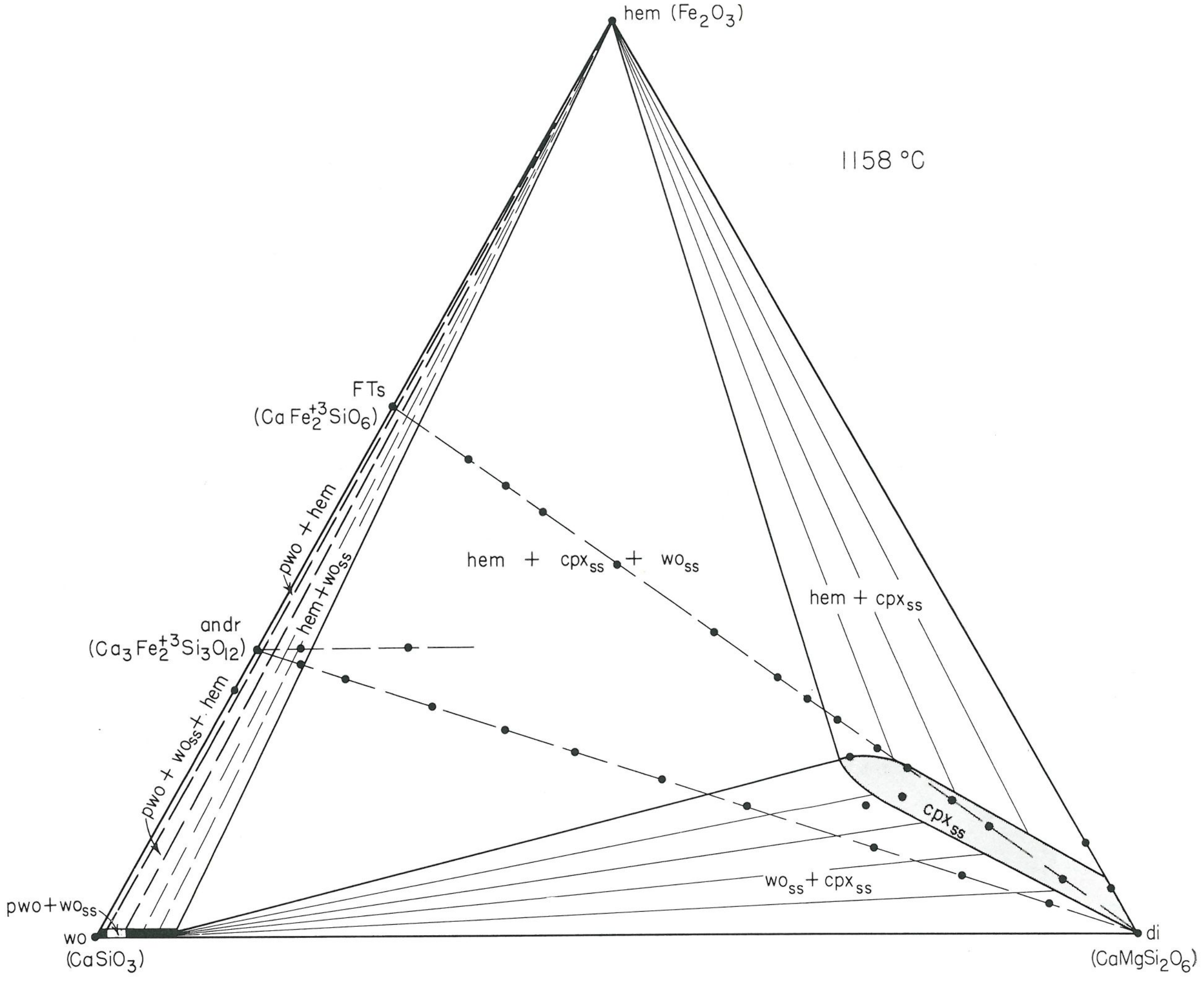

FIG. 11. Isothermal section of the diopside-wollastonite-hematite join at 1158°C.

*Isothermal section at 1158°C (Fig. 11).* At a temperature of 1158°C garnet is no longer stable, and all assemblages with andradite and its solid solutions are replaced by other phases. The assemblage andr$_{ss}$ + cpx$_{ss}$, with wo$_{ss}$ or with hem, is changed to hem + cpx$_{ss}$ + wo$_{ss}$. The assemblages hem + andr$_{ss}$, wo$_{ss}$ + andr$_{ss}$, and wo$_{ss}$ + pwo + andr$_{ss}$ are replaced by hem + wo$_{ss}$ or pwo, or both. The breakdown of andradite and its solid solutions does not effect a change of the di-rich part of the plane. Compared with the 1050° and 1137°C sections (Figs. 9 and 10) the clinopyroxene solid solution field is increased to about di$_{62}$wo$_{19}$hem$_{19}$, and also the range of compositions represented by hem + cpx$_{ss}$ as well as wo$_{ss}$ + cpx$_{ss}$ is expanded markedly.

*Isothermal (pseudoternary) section at 1250°C (Fig. 12).* At 1250°C the join di-wo-hem should probably not be treated as ternary but rather should be viewed in the context of the di-wo-hem-mt tetrahedron within the quinary system CaO-MgO-Fe$_2$O$_3$-FeO-SiO$_2$. However, the phase relationships may be elucidated from a ternary point of view when a pseudoternary plane di-wo-*iron oxides* of the di-wo-hem-mt tetrahedron is considered. Owing to this simplification phases labelled as *"iron oxides"* include hem or mt$_{ss}$, or both. Additional stable phases present are liquid, cpx$_{ss}$, pwo, and wo$_{ss}$.

## GEOLOGIC DISCUSSION

Results of this study illustrate the formation of ferridiopside solid solutions at magmatic temperatures. These findings are correlated with the observation that the rocks of the alkali basalt series are characteristically enriched in ferric iron. In general, most of the clinopyroxenes from olivine basalts, hawaiites, mugearites, basanites, and nephelinites contain small to moderate amounts of both the ferri-Tschermak's and acmite molecules. This can be deduced from clinopyroxene analyses given by Murray (1954), Brousse (1961), Yoder and Tilley (1962), Aoki (1964),

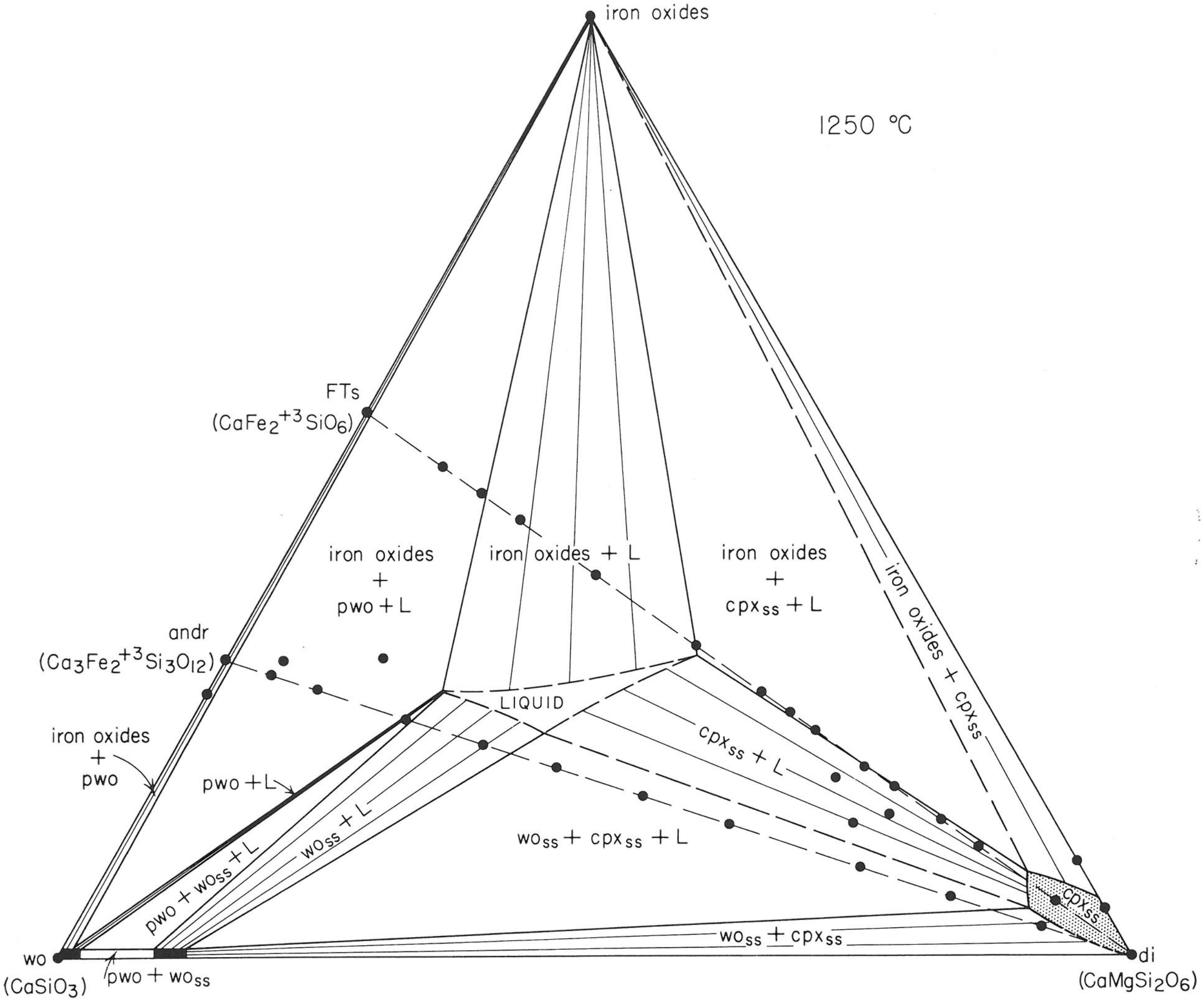

FIG. 12. Isothermal (pseudoternary) section of diopside-wollastonite-iron oxides at 1250°C. Phases labelled as "iron oxides" are either hem or $mt_{ss}$, or both.

Huckenholz (1965*a,* 1965*b,* and 1966), and Lewis (1967). High $P_{O_2}$ pressure in a normal alkali basalt magma or in its derivatives favors the solid solution of acmite in diopside (Yagi, 1966). With increasing sodium in excess of potassium in the bulk composition during fractionation, the acmite content in the clinopyroxenes increases as well, and the syenitic end member magmas precipitate aegirine or aegirine-augite under oxidizing conditions. The content of ferri-Tschermak's molecule in these clinopyroxenes is very small or absent, as may be seen from the data of Yagi (1953, 1966), Boesen (1964), Wilkinson (1966), and Tyler and King (1967).

Detailed information on alkaline rocks with potassic affinities and their related clinopyroxenes are rare. In general, the most common clinopyroxene in potassium-rich syenites, shonkinites, theralites, and ijolites is augitic in composition rather than acmitic. Closer relationships may be deduced from the potassium content of rocks and the composition of clinopyroxenes from the alkaline complex of Iron Hill, Colorado (Larsen, 1942). The potassium content usually exceeds that of sodium in the pyroxenite and melteigite members. Their related clinopyroxenes have average molecular compositions which can be expressed respectively as $di_{75}hd_{11}ac_2Ts_{12}$ and $di_{73}hd_{16}ac_2Ts_9$. The amount of the ferri-Tschermak's molecule in these clinopyroxenes is about 7 percent (max. 12%). The sodium content is larger in the ijolites, and a clinopyroxene of the composition $di_{68}hd_{18}ac_4Ts_{10}$ occurs containing 5 percent FTs. With further sodium enrichment in excess of potassium the clinopyroxene composition has changed to $di_{29}hd_{35}ac_{25}Ts_{11}$ and $di_{17}hd_{32}ac+jd_{43}Ts_8$ in the shonkinite and syenite end members, respectively. None or only traces of the ferri-Tschermak's molecule are present in these pyroxenes.

Additional data seem to support the view that clinopyroxenes from potassium-rich rocks are richest in ferri-Tschermak's molecule. Leucitite lavas from the 1929 eruption of Mount Vesuvius contain ferrian augites (Alfani, 1934; Müller, 1936) with an average amount of about 8 mole percent FTs. Augite found in a monchiquite from Khibina, Kola Peninsula (Lupanova, 1934) consists of 12 mole percent FTs; and Kashkai (1944) reported an augite from basaltic tuff in Azerbaidzhan with 10.4 percent. Ferrian augite is also found in a nepheline-bearing jacupirangite from Hesserau Hill, Quebec, close to the border of the Oka carbonatite complex (Gold, 1966). A clinopyroxene near Cape Tourmente, St. Joachim, Montmorency County, Quebec, has the largest amount of ferri-Tschermak's molecule in a natural specimen, 18.5 mole percent; and no sodium is reported in the chemical analysis given by Putman (1942). In summary, relatively larger amounts of the ferri-Tschermak's molecule of the clinopyroxenes are probably associated with those igneous rocks that have undergone strongly oxidizing conditions and contain only small amounts of either sodium or potassium, or both. The sodium deficiency prohibits the formation of relatively larger amounts of the acmite molecule, and potassium enters the diopside structure in very small amounts or nil.

The typical occurrence of andradite is in contact- or thermally metamorphosed, impure, calcareous sediments, and the assemblage andradite + clinopyroxene with either wollastonite or hematite is of particular interest with regard to the skarn deposits. The mineral assemblages obtained in the experiments under dry and oxidizing conditions are similar to those formed in nature from limestones and marbles. As examples, ferri-diopside is found in a thermally metamorphosed limestone of Juva, Finland (Juurinen and Hytönen, 1952), and almost pure andradite occurs in the marbles of the Hartenstein area (Moldanubian zone of Austria; Scharbert, 1966).

The phase relationships in the system diopside-wollastonite-hematite bear directly on the formation of andradite under magmatic conditions. Andradite is found in nepheline syenites, ijolites, and their volcanic equivalents, the phonolites and nephelinites. The andradite in these alkaline igneous rocks is generally the titaniferous variety, melanite or schorlomite, and the coexisting clinopyroxene is an aegirine-augite, aegirine, or diopside, occasionally rich in ferri-Tschermak's molecule. The main feature of those particular igneous rocks containing the mafic mineral association clinopyroxene, andradite, wollastonite, and iron ore (in most cases titanomagnetite, ilmenite, and occasionally hematite) is that andradite forms late in relation to the formation of clinopyroxene and wollastonite. This observation is supported by the petrographic descriptions of the alkaline rocks of the Iron Hill stock (Larsen, 1942), Alnö complex, Sweden (von Eckermann, 1948, 1958), Napak volcanoes, Uganda (King, 1949), Homa Bay area, Kenya (Pulfrey, 1950), Kaiserstuhl volcano (Wimmenauer, 1962), Magnet Cove alkaline complex, Arkansas (Erickson and Blade, 1963), and Oka carbonatite complex, Quebec (Gold, 1966). The thermal behavior of andradite outlined in the previous paragraphs is in accord with the formation of andradite in natural igneous rocks. Andradite does not crystallize on the liquidus nor appear with liquid in the system di-wo-hem. However, andradite having a Ti-bearing component in solid solution appears as a primary phase on the liquidus of the system enstatite-wollastonite-perovskite-hematite (Huckenholz, 1969). Its stability field is, therefore, well above the beginning of melting of alkali basalts, and it is likely to be a primary phase of mugearites and phonolites, which melt completely at temperatures below 1157°C.

## ACKNOWLEDGEMENTS

The first-named author is most grateful to the Deutscher Akademischer Austauschdienst for supporting a Fellowship at the Geophysical Laboratory of the Carnegie Institution of Washington. The manuscript was kindly reviewed by Drs. F. R. Boyd, Ikuo Kushiro, and Dean Presnall.

## REFERENCES

ALFANI, M. (1934) L'augite pneumatolitica raccolta sulle lave del fondo del cratere vesuviano nel 1929. *Per. Mineral. [Rome]*, **5**, 77–96.

AOKI, K. I. (1964) Clinopyroxenes from alkaline rocks of Japan. *Amer. Mineral.*, **49**, 1199–1223.

BOESEN, R. S. (1964) The clinopyroxenes of a monzonitic complex at Mount Dromedary, New South Wales. *Amer. Mineral.*, **49**, 1435–1457.

BOETTCHER, A. L. (1967) The Rainy Creek alkaline-ultramafic igneous complex near Libby, Montana. I. Ultramafic rocks and fenites. *J. Geol.*, **75**, 526–553.

BROUSSE, R. (1961) Minéralogie pétrographie des rochs volcaniques du Massif du Mont Dore (Auvergne), I-III. *Bull. Soc. Franc. Mineral. Cristallogr.* **84**, 131–156, 156–186, 245–259.

———, AND E. BOYER (1965) Grand cristaux d'augite dans une brèche volcanique intrusive. *Bull. Soc. Franc. Mineral. Cristallogr.*, **88**, 525–526.

CLARK, S. P., JR., J. F. SCHAIRER, AND J. DE NEUFVILLE (1962) Phase relations in the system $CaMgSi_2O_6$-$CaAl_2SiO_6$-$SiO_2$ at low and high pressure. *Carnegie Inst. Wash. Year Book*, **61**, 59–68.

COLEMAN, L. C. (1962) Effect of ionic substitution on the unit-cell dimensions of synthetic diopside. *In* A. E. J. Engel, H. L. James, and B. F. Leonard, Eds. *Petrologic Studies: A Volume in Honor of A. F. Buddington,* Geol. Soc. Amer., New York, p. 429–446.

ECKERMANN, H. VON (1948) The alkaline district of Alnö Island. *Sveriges Geol. Undersökn., Arsbok, Ser. Ca, Avhandl. Uppsat.*, **36**, 176 p.

——— (1958) The alkaline and carbonatite dikes of the Alnö formation on the mainland north-west of Alnö Island. *Kungl. Svenska Vetenskapsakad, Handl., Ser. 4,* **7**, no. 2, 61 p.

——— (1966) The pyroxenes of the Alnö carbonatite (sövite) and of surrounding fenites. *In Pap. Proc., Int. Mineral. Assoc., 4th Gen. Meet.,* Mineral. Soc. India, 126–139.

ERICKSON, R. L., AND L. V. BLADE (1963) Geochemistry and petrology of the alkalic igneous complex at Magnet Cove, Arkansas. *U. S. Geol. Surv. Prof. Pap.*, **425**, 95 p.

Ernst, W. G. (1966) Synthesis and stability relations of ferrotremolite. *Amer. J. Sci.*, **264**, 37–65.

Frechen, J. (1963) Kristallisation, Mineralbestand, Mineralchemismus und Förderfolge der Mafitite vom Dreiser Weiher, Eifel. *Neues Jahrb. Mineral., Monatsh.*, **1963**, 205–225.

Geller, S. (1967) Crystal chemistry of the garnets. *Z. Kristallogr.*, **125**, 1–47.

———, H. J. Williams, G. P. Espinosa, and R. C. Sherwood (1964) Importance of intrasublattice magnetic interactions and of substitutional ion type in the behavior of substituted yttrium iron garnets. *Bell Syst. Tech. J.*, **43**, 565–623.

Gold, D. P. (1966) The minerals of the Oka carbonatite and alkaline complex, Oka, Quebec. *Pap. Proc., Int. Mineral. Assoc., 4th Gen. Meet.*, Mineral. Soc. India, 109–125.

Huckenholz, H. G. (1965*a*) Der petrogenetische Werdegang der Klinopyroxene in den tertiären Vulkaniten der Hocheifel. I. Die Klinopyroxene der Alkaliolivinbasalt-Trachyt Assoziation. *Beitr. Mineral. Petrog.*, **11**, 138–195.

——— (1965*b*) Der petrogenetische Werdegang der Klinopyroxene in den tertiären Vulkaniten der Hocheifel. II. Die Klinopyroxene der Basanitoide. *Beitr. Mineral. Petrog.*, **11**, 415–448.

——— (1966) Der petrogenetische Werdegang der Klinopyroxene in den tertiären Vulkaniten der Hocheifel. III. Die Klinopyroxene der Pikritbasalte (Ankaramite). *Beitr. Mineral. Petrog.*, **12**, 73–95.

——— (1969) Synthesis and stability of Ti-andradite. *Amer. J. Sci., Schairer Vol.*, **267-A**, 209–232.

Ito, J., and C. Frondel (1967) Synthetic zirconium and titanium garnets. *Amer. Mineral.*, **52**, 773–781.

Juurinen, A., and K. Hytönen (1952) Diopside from Juva, Finland. *Bull. Comm. Géol. Finlande*, **157**, 145–146.

Kashkai, M.-A. (1944) The augites from Talysh (Azerbaidzhan). *Dokl. Akad. Nauk SSSR*, **43**, 351–353.

King, B. C. (1949) The Napak area of southern Karamoja, Uganda. *Uganda Geol. Surv. Mem.*, **5**, 57 p.

Larsen, E. S. (1942) Alkalic rocks of Iron Hill, Gunnison County, Colorado. *U. S. Geol. Surv. Prof. Pap.*, **197-A**, 1–64.

LeMaitre, R. W. (1962) Petrology of volcanic rocks, Gough Island, South Atlantic. *Geol. Soc. Amer. Bull.*, **73**, 1309–1340.

Lewis, J. F. (1967) Unit-cell dimensions of some aluminous natural clinopyroxenes. *Amer. Mineral.*, **52**, 42–54.

Lupanova, N. P. (1934) Basaltic hornblende and augite from monchiquite of Khibina Mountains. *Trudy Pétrog. Inst. Akad. Nauk SSSR*, **6**, 53–64.

Müller, K. (1936) Augit vom Vesuv. *Neues Jahrb. Mineral., Centralbl.*, **1936A**, 116–122.

Murray, R. J. (1954) The clinopyroxenes of the Garbh Eilean sill, Shiant Isles. *Geol. Mag.*, **91**, 17–31.

Phillips, B., and A. Muan (1960) Stability relations of iron oxides: phase equilibria in the system $Fe_3O_4$-$Fe_2O_3$ at oxygen pressures up to 45 atmospheres. *J. Phys. Chem.*, **64**, 1451–1453.

Presnall, D. C. (1966) The join forsterite-diopside-iron oxide and its bearing on the crystallization of basaltic and ultramafic magmas. *Amer. J. Sci.*, **264**, 783–809.

Pulfrey, W. (1950) Ijolitic rocks near Homa Bay, western Kenya. *Quart. J. Geol. Soc. (London)*, **105**, 425–459.

Putman, H.-M. (1942) Analyse chimique d'une augite du Cape Tourmente. *Naturaliste Can.*, **69**, 261–263.

Quareni, S., and R. de Pieri (1966) La struttura dell'andradite. *Mem. Accad. Patavina, Sci., Let., Arte, Cl. Sci. Mat. Nat.*, **78** (1956–1966).

Schairer, J. F., and N. L. Bowen (1942) The binary system $CaSiO_3$-diopside and the relations between $CaSiO_3$ and akermanite. *Amer. J. Sci.*, **240**, 725–742.

Scharbert, H. G. (1966) Andraditführende Einschaltungen im Marmor von Hartenstein (Kl. Kremstal, N. Ö.). *Neues Jahrb. Mineral., Montash.*, **1966**, 221–223.

Segnit, E. R. (1953) Some data on synthetic aluminous and other pyroxenes. *Mineral. Mag.*, **30**, 218–226.

Shapiro, L., and W. W. Brannock (1962) Rapid analysis of silicate, carbonate, and phosphate rocks. *U. S. Geol. Surv. Bull.*, **1144-A**, A1–A56.

Shepherd, E. S., and G. A. Rankin (with optical study by F. E. Wright) (1909) The binary systems of alumina with silica, lime and magnesia. *Amer. J. Sci.*, **28**, 293–333.

Simpson, E. S. W. (1954) The Okonjeje igneous complex, Southwest Africa. *Trans. Geol. Soc. S. Afr.*, **57**, 125–166.

Skinner, B. J. (1956) Physical properties of end-members of the garnet group. *Amer. Mineral.*, **41**, 428–436.

Swanson, H. E., M. I. Cook, T. Isaacs, and E. H. Evans (1960) Standard X-ray diffraction powder patterns. *U. S. Nat. Bur. Stand. Circ.*, **539**, (vol. 9), 22–23.

Taylor, H. P., J. Frechen, and E. T. Degens (1967) Oxygen and carbon isotope studies of carbonatites from the Laacher See district, West Germany, and the Alnö district, Sweden. *Geochim. Cosmochim. Acta*, **31**, 405–430.

Tilley, C. E., and J. Gittins (1961) Igneous nepheline bearing rocks of the Haliburton-Bancroft province of Ontario. *J. Petrology*, **2**, 38–48.

Tyler, R. C., and B. C. King (1967) The pyroxenes of the alkaline igneous complexes of eastern Uganda. *Mineral. Mag.*, **36**, 5–21.

Vilminot, J. C. (1965) Les enclaves de peridotite et de pyroxenolite dans le basalte du Rocher du Lion. *Bull. Soc. Franc. Mineral. Cristallogr.*, **88**, 109–118.

Wilkinson, J. F. G. (1957) The clinopyroxenes of a differentiated teschenite sill near Gunnedah, New South Wales. *Geol. Mag.*, **94**, 123–133.

——— (1966) Clinopyroxenes from the Square Top intrusion, Nundle, New South Wales. *Mineral. Mag.*, **35**, 1061–1070.

Wimmenauer, W. (1962) Beiträge zur Petrographie des Kaiserstuhls. Teil IV. Die Gesteine der phonolithischen Familie. Teil V. Die subvulkanischen Breccien. *Neues Jahrb. Mineral., Abhandl.*, **98**, 367–415.

Yagi, K. (1953) Petrochemical studies of the alkalic rocks of the Morotu district, Sakhalin. *Geol. Soc. Amer. Bull.*, **64**, 769–810.

——— (1966) The system acmite-diopside and its bearing on the stability relations of natural pyroxenes of the acmite-hedenbergite-diopside series. *Amer. Mineral.*, **51**, 976–1000.

Yoder, H. S., Jr., and C. E. Tilley (1962) Origin of basalt magmas: an experimental study of natural and synthetic rock systems. *J. Petrology*, **3**, 342–532.